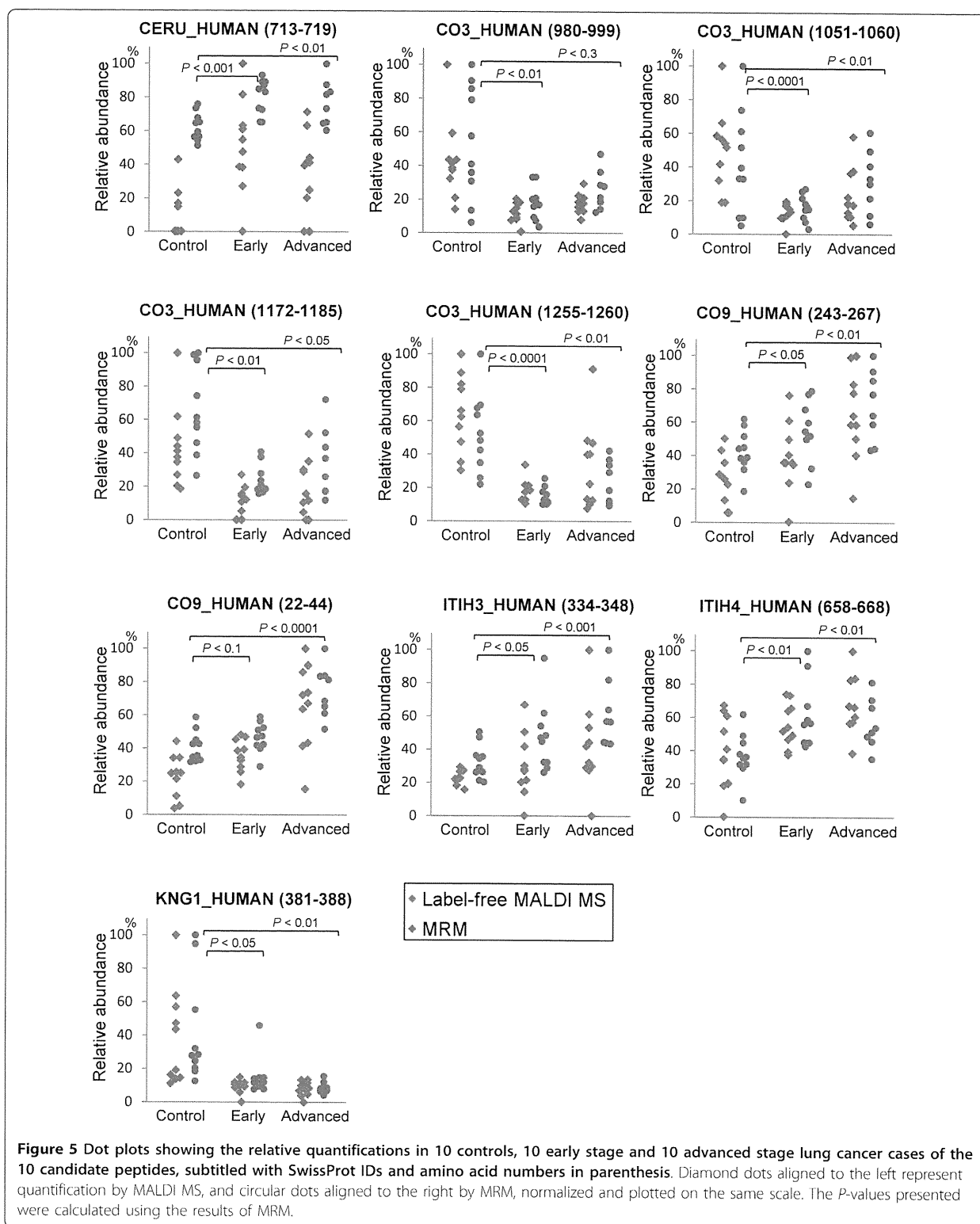


Table 1 List of lung cancer biomarker candidates screened by label-free MALDI MS and their verification result on MRM.

Uniprot ID	Protein Name	Peptide Sequence	MALDI MS		MRM		Correlation Coefficient
			t-test †	Log2 (LC/Control)	t-test †	Log2 (LC/Control)	
P04217	Alpha-1B-glycoprotein	CEGPIPDVTFELLREGETKAVK	-	0.67	-	-	-
		FALVREDR	3.8E-03	-0.38	0.13	0.24	0.315
P01011	Alpha-1-antichymotrypsin	EQLSLLDRFTEDAK	1.4E-03	0.80	0.077	0.33	0.106
		FTEDAKRLRYGSEAFATDFQDSAAAK	4.6E-03	0.58	-	-	-
		PQDTHQSR	5.6E-03	0.84	-	-	-
P43652	Afamin	DGLKYHYLIR	1.1E-03	-0.93	-	-	-
P02746	Complement C1q subcomponent subunit B	GNLCVNLMR	6.5E-03	0.87	-	-	-
P00736	Complement C1r subcomponent	CLPVCCKPVPNPVEQR	-	0.42	-	-	-
		DYFIATCK	6.9E-03	0.49	0.15	0.14	-0.238
P00450	Ceruloplasmin	YTVNQCR	0.017	1.1	3.1E-04	0.29	0.411*
P10909	Clusterin	YVNKEIQNAVNGVK	0.01	0.33	0.19	-0.87	-0.015
P06681	Complement C2	TAVDHIREILNINQK	2.7E-03	1.4	0.051	0.23	N/A
P01024	Complement C3	AGDFLEANYMNLQR	5.9E-05	-1.4	3.8E-04	-1.3	0.690**
		ILLOGTPVAQMTEDAVIDAER	2.1E-04	-1.3	0.019	-0.87	0.448*
		KGYTQQLAFR	2.8E-03	-1.1	3.9E-05	-1.3	0.800**
		QPSSAFAAFVKR	6.7E-03	-1.3	2.0E-03	0.24	-0.455
		WLNEQR	2.5E-03	-1.0	7.8E-06	-1.5	0.521**
P01031	Complement C5	FWKDNLQHKDSSVPNTGTAR	0.012	0.67	-	-	-
		TLRWPEGVKR	0.066	0.80	-	-	-
P13671	Complement component C6	IEEADCKNKFR	0.011	1.2	-	-	-
P10643	Complement component C7	VFSGDGKDFYR	9.5E-03	0.81	-	-	-
P02748	Complement Component C9	FTPTETNKAEQCCEETASSISLHGK	2.4E-04	1.4	6.1E-03	0.49	0.472*
		QYTgTSYDPELTESTSSASHIDCR	1.9E-03	1.1	3.8E-03	0.57	0.769**
P22792	Carboxypeptidase N subunit 2	SQCTYSNPEGTIVLACDQAQCR	1.4E-03	0.56	0.062	0.16	0.372
P00748	Coagulation factor XII	CTHKGRPGPQWCATTPNFDQDQR	4.3E-03	1.2	-	-	-
Q9UGM5	Fetuin-B	MSPPQLALNPSALLSR	3.0E-03	0.62	0.03	0.58	0.189
P02751	Fibronectin	AQITGYR	1.1E-03	-0.47	0.077	-0.18	0.774**
		GFNCESKPEAEETCFDKYTGNTYR	1.9E-03	-0.69	0.42	-0.11	0.146
		IGFKLGVRRPSQGGAPR	5.7E-03	-0.90	-	-	-
P26927	Hepatocyte growth factor-like protein	RVDRLDQR	6.1E-03	-0.57	0.013	0.38	-0.128
P18065	Insulin-like growth factor-binding protein 2	LAACGPPPVAPPAVAVAAGGAR	2.5E-03	0.67	-	-	-
Q06033	Inter-alpha-trypsin inhibitor heavy chain H3	EHLVQATPENLQEAR	4.6E-03	0.97	3.6E-03	0.65	0.578**
Q14624	Inter-alpha-trypsin inhibitor heavy chain H4	EKNGIDIYSLTVDSR	4.7E-04	0.65	0.062	0.40	0.368
		ETLFSVMPGLK	-	0.09	0.01	0.42	0.331
		MNFRPGVLSSR	9.8E-03	0.40	1.0E-03	0.63	0.413*
		SPEQQETVLDGNLIIRYDVDR	0.013	1.2	-	-	-
P03952	Plasma kallikrein	CQFFTYSLLPEDCKEEKCK	-	-0.32	-	-	-
P01042	Kininogen-1	RPPGFSPF	2.0E-04	-2.0	5.1E-04	-1.74	0.876**
P27918	Properdin	TCNHPVPOHGGPFCAGDATR	7.2E-04	-0.52	-	-	-
Q13103	Secreted phosphoprotein 24	DSGEDPATCAFQR	3.7E-03	-0.53	-	-	-

†: "-" indicates candidate screened by present/absent search,
 ‡: "-" indicates no MRM data obtained, *: $P < 0.05$, **: $P < 0.01$,
 g: indicates site of O-linked glycosylation.
 N/A: valid value too small for calculation of correlation threshold.



39 kDa subunit of C3 protein was strongly suppressed in early-stage patients (Figure 6A). Since this subunit was also detected by the monoclonal antibody raised against C3d fragment (Figure S-2 Additional File 1), the 39 kDa subunit was assigned to be C3dg fragment [17]. This fragment encompasses all of the four C3 peptide candidates identified by LC-MALDI screening, and semi-quantitative analysis of the immunoblot (Figure 6B) almost exactly reproduced the screening result. Moreover, C3dg fragment was shown to escape immunodepletion by MARS-Hu14 column (Figure S-2). Therefore, the apparent difference in complement C3 abundance observed in the screening was reflecting the degree of proteolytic degradation associated with lung cancer.

Finally, the benefit of deglycosylation in this biomarker screening was assessed by mining the candidate peptides from the control experiment (comparing deglycosylated and untreated serum) and verifying whether or not deglycosylation facilitated biomarker identification. Figure 7 shows the levels of complement component C9 peptides in the control experiment, which were clearly overrepresented by deglycosylation. Notably, the signal intensity of non-glycopeptide (243-267) was doubled, reiterating the observation that non-glycopeptide was

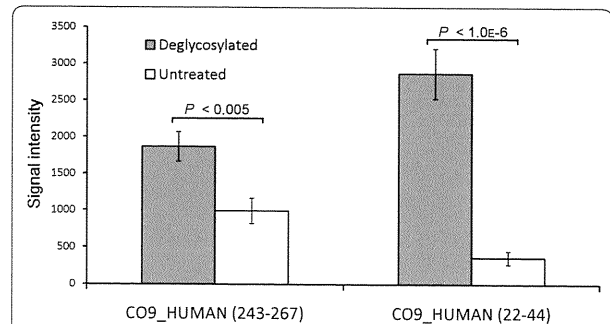


Figure 7 Bar chart representing the signal intensities of complement component C9 peptides detected from the tryptic digest of deglycosylated serum (filled bars) and untreated serum (open bars), $n = 6$. The numbers in parenthesis are amino acid numbers: 243-267 corresponds to $_{243}$ FPPTETNKAEQCCEETASSISLHG $_{267}$ K and 22-44 corresponds to $_{22}$ QYTgTSYDPELTSSGASHIDC $_{44}$ R, where "g" represents the site of O-linked glycan attachment. Error bars are one standard deviation.

also subject of signal enhancement by deglycosylation. Moreover, the signal intensity of peptide (22-44) was increased by 10-fold. Since this peptide was identified as O-linked glycopeptide (attachment of N-acetylgalactosamine and galactose as predicted from the m/z shift), the addition of sialidase probably contributed to reduction of glycan complexity and increased ionization efficiency. The sialylated counterpart was not detected in the untreated control.

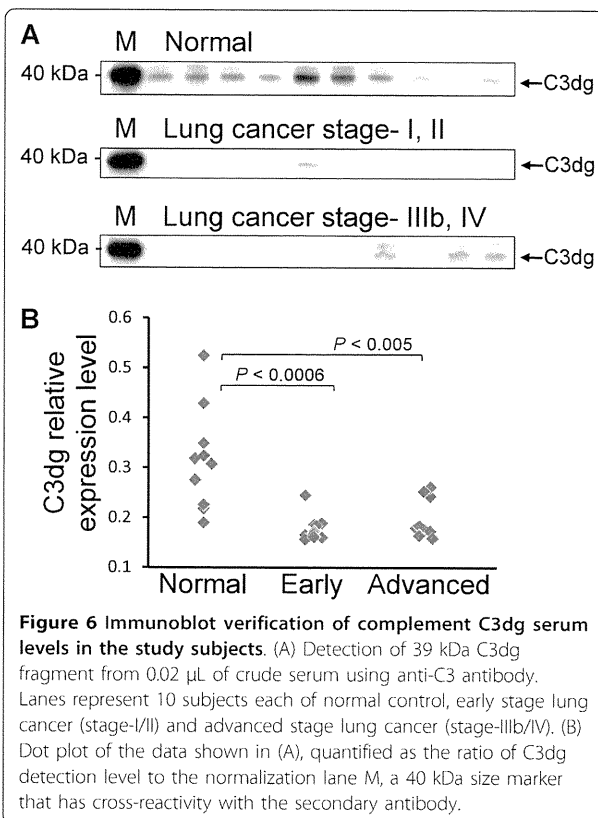


Figure 6 Immunoblot verification of complement C3dg serum levels in the study subjects. (A) Detection of 39 kDa C3dg fragment from 0.02 μ L of crude serum using anti-C3 antibody. Lanes represent 10 subjects each of normal control, early stage lung cancer (stage-I/II) and advanced stage lung cancer (stage-IIIb/IV). (B) Dot plot of the data shown in (A), quantified as the ratio of C3dg detection level to the normalization lane M, a 40 kDa size marker that has cross-reactivity with the secondary antibody.

Discussion

The aim of this study was to introduce deglycosylation as a facile and universal sample preparation step in shotgun proteomic analysis because we expected that the undermining effect exerted by the large proportion of glycopeptides was more extensive than previously considered. Therefore, for the first time, we have performed a direct comparison between deglycosylated and untreated serum samples, and showed that deglycosylation actually results in improvement of the shotgun peak profile. This was observed in terms of both acquisition of unique peaks and enhancement of existing peaks.

The acquisition of unique peaks by deglycosylation was expected, as it is widely recognized that deglycosylated peptides have much higher ionization efficiency than the corresponding glycopeptides [18,19]. It is well established that deglycosylation results in the detection of "new" peaks and increases the depth of information acquired by shotgun analysis [20,21]. However, this study revisited the same phenomenon from different perspective. Our novel finding was that signal enhancement by deglycosylation extended up to 8% of existing non-glycopeptide peaks (Figure 3). This result strongly suggested that there was notable ionization suppression effect exerted by glycopeptides on co-existing analytes,

and that signal intensities were enhanced through alleviation of suppression in deglycosylated sample. Incorporation of ^{18}O into the site of deglycosylation by H_2^{18}O was utilized to facilitate the identification of glycopeptides. The potential pitfalls of this approach as pointed out by Angel et al. [22] was circumvented by performing deglycosylation before tryptic digestion, and our data showed that 73% of identified glycopeptides fulfilled the biological consensus NxT/S. This strategy helped to confirm that only a small proportion of peaks that were enhanced by deglycosylation were actually glycosylated. We further demonstrated the evidence that deglycosylation improves the reproducibility of replicate measurements to some extent (Figure 4). The level of technical variability, median CV of 31%, was comparable to previously reported label-free quantification methods based on LC-ESI-MS [8] or LC-MALDI MS [16].

Unfortunately, previous studies on ionization suppression effects had mainly focused on selective detection of glycopeptides in mixtures of peptides [23], and cannot explain the phenomenon addressed here. Separate investigation needs to be conducted in order to elucidate the mechanism and the extent to which glycopeptides interfere with the ionization of co-existing peptides.

Serum deglycosylation coupled with label-free quantification was applied to biomarker screening for lung cancer and led to the identification of unique biomarker candidates including the fragmentation state of complement C3, complement component C9 peptide with novel O-linked carbohydrate and Kininogen-1 peptide with C-terminal Phe [24]. The benefit of deglycosylation in the biomarker screening was demonstrated by enhanced detectability of the complement component C9 peptides, particularly for O-linked glycopeptide whose intact form with sialic acid was hardly detected. Since many O-linked glycans contain sialic acid, the data presented here demonstrates a high potential of sialidase usage for comprehensive analysis of O-linked glycans.

As with other label-free quantitative proteomics, more proteins were quantified by single peptide than those quantified by multiple peptides [25] due to the high technical variability associated with label-free shotgun analysis. Therefore, we employed MRM to complement the screening by MALDI MS with the aim of eliminating false-positive results. This approach successfully ruled out many candidates while retaining confident candidates, as verified by western blotting experiment of complement C3.

Complement C3 is the major component of the classical complement pathway. Upon antigenic stimulation, C3 convertase cleaves C3 into C3a and C3b, which subsequently triggers reaction cascade leading to the formation of membrane attack complex, by either the classical

or alternative pathway [17]. C3a contains a multiply interacting motif known as anaphylatoxin [26]. Recently, a number of proteomic studies have identified C3a as biomarker candidates for colon cancer [27], chronic hepatitis C and related hepatocellular carcinoma [28], insulin resistance/type-2 diabetes [29] and chronic lymphoid malignancies [30]. While upregulation of C3a is widely reported and interpreted as an indicator of primary inflammatory response, there is limited association reported between C3dg and cancer. C3dg is known as the ligand of complement receptor 2 [31] and may be critically involved in cancer recognition. The mechanism by which the production of C3dg is suppressed in response to the onset of lung cancer requires further investigation.

In the Expressionist label-free quantification platform employed here, peptide peak clusters are defined by retention time-*m/z* coordinate on the 2D-map, enabling quantitative analysis without MS/MS information that were essential in other platforms [32-35]. The feature that provides the ground for this concept is perfect alignment of mass chromatograms in the retention time dimension because slight drift is unavoidable even in well-optimized separation system. In this respect, Expressionist demonstrated spectacular computational strength. The range of retention time drift in the 30 LC-MALDI analyses performed in this study was from -5 minutes to +5 minutes, a maximum of 10 minutes deviation, but the software was still capable of good alignment without any obvious retention time mismatch (data not shown). Therefore, variation in experimental conditions, such as changing the analytical column lot, should easily be tolerated. This feature enables integration of several, even retrospective, analyses, which is needed for the continuous pursuit for biomarker identification and validation.

Moreover, being a server-based module, Expressionist has greater data processing capability than other stand-alone software. This is another advantageous feature because, in general, attempts to increase proteome coverage involve vast increase in data amount, whether it be a multi-dimensional fractionation strategy [36,37] or an extremely long gradient separation [38]. Importantly, considering the fact that low-abundance analytes are more prone to ionization suppression [39], we speculate that the benefits of sample deglycosylation we addressed here would take greater effect with increasing dynamic range of detection. Such in-depth label-free analysis is currently not available, however, we demonstrated herein that current technology is already capable of large-scale label-free analysis, and we addressed its potentiality as a biomarker discovery platform. Taken together, we believe that sample deglycosylation will prove to be a valuable sample preparation protocol in

shotgun proteomic analysis in near future for analyzing glycoprotein-rich samples.

Conclusions

The studies described herein demonstrated that serum deglycosylation has positive effect on both data content and reproducibility through production of deglycosylated peptides and possibly through alleviation of ionization suppression by intact glycopeptides. The results therefore suggested the role of deglycosylation as a simple, indispensable method to improve the general performance of label-free quantification. Its first application to serum proteomic profiling by label-free LC-MALDI MS demonstrated that this strategy could lead to the identification of unique candidates, which could be effectively applied to any samples with high glycoprotein contents, such as other clinical body fluids, membrane proteomics or secretome analysis.

Methods

Reagents

Trizma base pH 8.3, iodoacetamide, ammonium bicarbonate, ammonium citrate, formic acid were purchased from Sigma (Saint Louis, MO). PlusOne grade SDS and dithiothreitol (DTT) were purchased from GE Healthcare (Uppsala, Sweden). CHAPS was purchased from Chemical Dojin (Kumamoto, Japan). N-glycosidase F was purchased from Roche (Basel, Switzerland). α 2-3,6,8,9-neuraminidase was purchased from Merck (Darmstadt, Germany). Trypsin Gold was purchased from Promega (Madison, WI). $H_2^{18}O$ was supplied from Cambridge Isotope Laboratories Inc. (Andover, MA). Alpha-cyano-4-hydroxycinnamic acid (CHCA) was purchased from Shimadzu-GLC (Kyoto, Japan). LC/MS grade acetonitrile and 25% trifluoroacetic acid (TFA) were purchased from Wako Pure Chemicals (Osaka, Japan).

Serum Samples

Archived human serum samples were obtained with informed consent from 20 patients with lung adenocarcinoma and at Hiroshima University Hospital. Serum samples as normal controls were also obtained with informed consent from 13 healthy volunteers who received medical checkup at Hiroshima University Hospital (Table S-1, Additional File 1). Serum was collected using standard protocol from whole blood by centrifugation at $1500 \times g$ for 10 min and stored at $-150^\circ C$. This study was approved by individual institutional ethical committees.

Immunodepletion

20 μL serum aliquots obtained from healthy volunteer were subjected to Multiple Affinity Removal System

(Hu-14, 4.6 mm \times 100 mm, Agilent Technologies, Santa Clara, CA) according to the manufacturer's protocol using a conventional HPLC system (Shimadzu Corp., Kyoto, Japan). The flow-through fraction was desalted with a protein separation column (mRP-C18, 4.6 mm \times 50 mm, Agilent Technologies). Desalted serum proteins were dried with a SpeedVac evaporator.

Deglycosylation

All solutions in the following deglycosylation step were freshly prepared with $H_2^{18}O$. Protein aliquots were dissolved in 12.5 μL of 2% SDS, 20 mM DTT, 20 mM Trizma-base pH 8.3 and heated to $100^\circ C$ for 5 minutes. After cooling, 25 μL of 10% CHAPS, 83.4 μL 20 mM Trizma-base pH 8.3, 1 μL N-glycosidase F and 0.6 μL α 2-3,6,8,9-neuraminidase were added in the written order with thorough mixing. $H_2^{18}O$ was added in place of the enzymes for "untreated" samples. The reaction mixture was incubated at $37^\circ C$ overnight.

Tryptic digestion

Deglycosylated proteins were reduced by 10 mM DTT and incubated at $56^\circ C$ for 15 minutes, followed by alkylation by 50 mM iodoacetamide at ambient temperature for 45 minutes in dark. 20% of the total reaction mixture was purified by SDS-PAGE, applying voltage until all of the proteins had entered the separating gel. Whole lanes were cut out and subjected to in-gel tryptic digestion. Briefly, gel slices were cut into small pieces and were washed 3 times in 30% acetonitrile 50 mM ammonium bicarbonate before digesting with 200 ng of trypsin in 100 μL 50 mM ammonium bicarbonate at $37^\circ C$ overnight. Peptides were extracted by 2 rounds of 50% acetonitrile and 100% acetonitrile washes. Recovered peptides were dried in SpeedVac and reconstituted in 10 μL of 2% acetonitrile 0.1% TFA for LC-MALDI analysis.

LC-MALDI Analysis

Serum tryptic digest with or without deglycosylation was separated using DiNa nano-HPLC system (KYA Technologies, Tokyo, Japan). Solvent A was 2% acetonitrile and 0.1% TFA in water and solvent B was 70% acetonitrile and 0.1% TFA in water. 2 μL sample, a final amount equivalent to 0.4 μL serum, was injected onto a trap column (L-column ODS, 5 μm , 0.3×5 mm, CERI, Saitama, Japan) and loaded by 8 $\mu L/min$ flow of solvent A. At 5 min, valve was switched and the peptides were separated by an in-house packed analytical column (L-column ODS, 3 μm , in 0.1 mm \times 200 mm capillary) at 200 nL/min flow rate using the following gradient: 5 min, 2% solvent B; 6 min, 10% solvent B; 90 min, 55% solvent B; 95 min, 100% solvent B; and 110 min, 100% solvent B. The column end was connected directly to the spotting tip of DiNA MAP target plate spotting

device (KYA Technologies). CHCA matrix solution was prepared at 1.5 mg/mL concentration in 70% acetonitrile, 0.1% TFA and 0.03 mg/mL ammonium citrate, which was pumped to the spotting tip at 2.2 μ L/min flow rate and therein mixed with column elution. The mixture was deposited onto a 1536-well μ Focusing plate (Hudson Surface Technologies Inc., Newark, NJ) every 15 seconds between 20.0 to 109.75 minutes for a total of 360 spot fractions. Mass spectrometric analysis was performed using 4800 Plus MALDI TOF/TOF Analyzer (AB Sciex, Foster City, CA) operated on 4000 Series Explorer software version 3.5. For each fraction spot, data was accumulated from 1000 laser shots in a randomized raster of 400 μ m diameter over mass range m/z 800-4000. The laser repeat rate was 200 Hz and the laser power was fixed at 3500 units throughout the experiment. 5 calibration spots comprising 6 standard peptides were used for external calibration.

Data analysis

Individual MALDI MS raw data was exported as t2d file, ordered in chromatographic order and imported into Expressionist Refiner MS system (Genedata AG, Basel, Switzerland), where they were combined and displayed as mass chromatograms. Default processing parameters were applied unless otherwise specified. The chromatogram data was first simplified by subtracting the background noise by using the following criteria: 0.3 min RT window, 40% quantile subtraction, 0.15 point RT smoothing. After subtraction, all data points below threshold intensity of "100" were clipped to zero. A set of chromatograms were then aligned in the RT direction by nonlinear transformation, mapping the original time onto a common universal retention time, to ensure that equal RT values correspond to the elution of the same compounds. The following parameters were applied: RT transformation window, 5 min; RT search interval, 30 min; m/z window, 0.2 Da; gap penalty, 1. Peak signals were detected by summed peak detection algorithm, which computes a temporary averaged chromatogram over all input chromatograms, thereby allowing them to share the matching set of peaks with identical boundaries. Here, the summation windows of 0.2 Da in the m/z direction and 1 minute in the RT direction were selected. The detected peaks were grouped into isotopic clusters of individual compounds by summed isotope clustering activity, using the following parameters: minimum charge, 1; maximum charge, 2; maximum missing peaks, 1; first allowed gap position, 3; RT window, 1 min; peptide isotope shaping tolerance, 0.8.

Statistical analysis

The cluster information generated by Refiner MS was imported into Genedata Expressionist Analyst software

for statistical analysis. The clusters were first filtered by a valid value proportion of 100% (i.e. signal was detected in all of the experimental replicates). All of these clusters were subjected to t-test for extracting differentially expressed clusters between the experimental groups, where $P < 0.01$ was considered to be significant. Present/absent search was performed to select for clusters with 0 or 1 counterpart detection, which were omitted by t-test.

Protein identification

As an exhaustive study, full MS/MS analysis was performed on three of the replicate runs. Precursor peaks were selected according to the software interpretation algorithm, while limiting the maximum number of acquisition to 10 per spot. Precursor peaks were measured in descending order of intensity. Precursor ions were isolated at 150 FWHM resolution, fragmentation was induced without the use of collision gas at 6 kV and fragment ions were further accelerated at 15 kV. Laser power of 4200 units was used, and the acquisition was summed over 2000 laser shots or until 4 fragment peaks exceeded S/N 100. Protein Pilot software version 2.0 was used to generate MS/MS peak lists for searching by MASCOT [32] version 2.2.03 (Matrix Science, London, U.K.) against 20345 human sequences of SwissProt version 57.14. Prior to search, a custom +3 Da modification on asparagine residue resulting from deglycosylation in $H_2^{18}O$ was defined. The search parameters were as follows: enzyme, trypsin (allow up to 2 missed cleavages); fixed modification, carbamidomethyl; variable modifications, ^{18}O -deglycosylation (Asn); peptide tolerance, 300 ppm; MSMS tolerance, 0.5 Da. Ion expectation score of 0.05 was used for the cut-off line for identification. For candidate biomarker peptides that were not identified by this method, searching was iteratively repeated in different search parameters, such as "semitrypsin" enzyme restriction, "N-terminal pyroglutamic acid" and "+365 Da modification on Thr" (corresponding to O-linked N-acetylhexosamine and hexose attached to a threonine residue) as variable modifications.

Multiple reaction monitoring

2 μ L of the serum tryptic digest analyzed by LC-MALDI was diluted by adding 6 μ L of solvent A and 4 μ L of tBSA proteomic standard (KYA Technologies) dissolved at 50 fmol/ μ L. 1 μ L of this mixture was injected for a single analysis. Paradigm nano-HPLC system with PAL autoinjector was used for separation. Solvent A was 2% ACN in 0.1% formic acid, solvent B was 90% ACN in 0.1% formic acid, and sample was loaded with 2% ACN in 0.1% TFA. The trap column was L-column ODS, 5 μ m, 0.3 \times 5 mm, and the analytical column was L-column ODS loaded in-house directly into a sprayer tip (GL Science, Tokyo, Japan).

MRM was performed using 4000QTRAP mass spectrometer (AB Sciex) during a 13 minutes gradient (2-55% solvent B) at 200 nL/min flow rate. 70 ions were monitored simultaneously for 30 minutes, each transition with 20 ms dwell time with 5 ms interval, taking a total of 1.75 s per scan. Transitions were selected from series of pilot experiment in which in-silico developed transitions for each peptide were tested for signal intensity and specificity. Transitions were considered as the derivative of target peptide only when all of them responded simultaneously and the retention time of detection matched that of LC-MALDI data. Instrument settings were as follows: declustering potential, 70; entrance potential, 10; curtain gas, 10; collision gas, 4; ion spray voltage, 2100; ion source gas, 10; interphase heater temperature, 150°C. Peak areas were integrated using MultiQuant software version 1.1.0.26. Raw data was normalized to the total signal acquired, which includes two spiked-in BSA fragments detected at highest intensity.

Immunoblot analysis

For the verification study, crude serum samples from fresh aliquots for all screening sample set (except for 3 normal controls N-3, 4, and 10, which were substituted by N-11, 12, and 13, respectively) were analyzed. 0.5 µL of crude serum was diluted 100-fold with SDS-PAGE sample buffer, boiled and 20 µL was used for immunoblot analysis. SDS-PAGE was performed using NuPAGE Bis-Tris 4-12% acrylamide gel with 2-morpholinoethanesulfonic acid buffer system, and electroblotted onto a PVDF membrane. The blots were probed with anti-C3 polyclonal antibody (Sigma, product code GW20073F) diluted 5000-fold in 5% skim milk, followed by incubation with horseradish peroxidase-conjugated secondary antibody (Sigma, product code A9046) diluted 10000-fold in 2% BSA. The reactivity was visualized on X-ray films using ECL detection kit (GE Healthcare). Immunoblot was also performed with anti-C3d monoclonal antibody (Abbiotec, San Diego, CA) and horseradish peroxidase-conjugated secondary antibody (GE Healthcare) to confirm specificity of the polyclonal antibody (Figure S-2).

Additional material

Additional file 1: Supplementary Information. This PDF file contains the following material: Figure S-1, a histogram and summary of the number of reproducible peaks. Figure S-2, an immunoblot showing the specificity of antibodies used. Table S-1, the list of serum samples. Table S-2, the list of glycopeptides identified in this study. Table S-3, the detail of MRM transitions used for verification analysis.

Author details

¹Graduate School of Frontier Sciences, The University of Tokyo, Kashiwanoha5-1-5, Chiba, Japan. ²Laboratory for Biomarker Development,

Center for Genomic Medicine, RIKEN, Tsurumiku-Suehirocho1-7-22, Yokohama, Japan. ³Laboratory of Molecular Medicine, Human Genome Center, Institute of Medical Science, The University of Tokyo, Shirokanedai4-6-1, Tokyo, Japan. ⁴Department of Molecular and Internal Medicine, Hiroshima University, Minamiku-Kasumi1-2-3, Hiroshima, Japan. ⁵Shimadzu Corporation, Nishinkyō-Kuwabaracho1, Kyoto, Japan.

Authors' contributions

AT performed all experiments and drafted the manuscript. HN and KM added statistical interpretation. NI and NK provided the serum samples and revised the manuscript. YD and TAS contributed to mass spectrometry analysis. YN critically revised the manuscript. KU conceived the study, helped in experimental design and critically revised the manuscript. All authors read and approved the final manuscript.

Competing interests

This study is supported in part by the grants from Toppan Printing Co., Ltd., Tokyo, Japan, and Shimadzu Corporation, Kyoto, Japan.

Received: 8 December 2010 Accepted: 8 April 2011

Published: 8 April 2011

References

1. Anderson NL, Anderson NG: The human plasma proteome: history, character, and diagnostic prospects. *Mol Cell Proteomics* 2002, **1**:845-867.
2. Ong SE, Mann M: Mass spectrometry-based proteomics turns quantitative. *Nat Chem Biol* 2005, **1**:252-262.
3. Gygi SP, Corthals GL, Zhang Y, Rochon Y, Aebersold R: Evaluation of two-dimensional gel electrophoresis-based proteome analysis technology. *Proc Natl Acad Sci USA* 2000, **97**:9390-9395.
4. Kuyama H, Watanabe M, Toda C, Ando E, Tanaka K, Nishimura O: An approach to quantitative proteome analysis by labeling tryptophan residues. *Rapid Commun Mass Spectrom* 2003, **17**:1642-1650.
5. Ong SE, Blagoev B, Kratchmarova I, Kristensen DB, Steen H, Pandey A, Mann M: Stable isotope labeling by amino acids in cell culture, SILAC, as a simple and accurate approach to expression proteomics. *Mol Cell Proteomics* 2002, **1**:376-386.
6. Ross PL, Huang YN, Marchese JN, Williamson B, Parker K, Hattan S, Khainovski N, Pillai S, Dey S, Daniels S, *et al*: Multiplexed protein quantitation in *Saccharomyces cerevisiae* using amine-reactive isobaric tagging reagents. *Mol Cell Proteomics* 2004, **3**:1154-1169.
7. Schulze WX, Usadel B: Quantitation in Mass-Spectrometry-Based Proteomics. *Annu Rev Plant Biol* 2010.
8. Wang W, Zhou H, Lin H, Roy S, Shaler TA, Hill LR, Norton S, Kumar P, Anderle M, Becker CH: Quantification of proteins and metabolites by mass spectrometry without isotopic labeling or spiked standards. *Anal Chem* 2003, **75**:4818-4826.
9. Bondarenko PV, Chelius D, Shaler TA: Identification and relative quantitation of protein mixtures by enzymatic digestion followed by capillary reversed-phase liquid chromatography-tandem mass spectrometry. *Anal Chem* 2002, **74**:4741-4749.
10. Omenn GS, States DJ, Adamski M, Blackwell TW, Menon R, Hermjakob H, Apweiler R, Haab BB, Simpson RJ, Eddes JS, *et al*: Overview of the HUPO Plasma Proteome Project: results from the pilot phase with 35 collaborating laboratories and multiple analytical groups, generating a core dataset of 3020 proteins and a publicly-available database. *Proteomics* 2005, **5**:3226-3245.
11. Zhang H, Li XJ, Martin DB, Aebersold R: Identification and quantification of N-linked glycoproteins using hydrazide chemistry, stable isotope labeling and mass spectrometry. *Nat Biotechnol* 2003, **21**:660-666.
12. Liu T, Qian WJ, Gritsenko MA, Camp DG, Monroe ME, Moore RJ, Smith RD: Human plasma N-glycoproteome analysis by immunoaffinity subtraction, hydrazide chemistry, and mass spectrometry. *J Proteome Res* 2005, **4**:2070-2080.
13. Kaji H, Saito H, Yamauchi Y, Shinkawa T, Taoka M, Hirabayashi J, Kasai K, Takahashi N, Isobe T: Lectin affinity capture, isotope-coded tagging and mass spectrometry to identify N-linked glycoproteins. *Nat Biotechnol* 2003, **21**:667-672.
14. Constantopoulos TL, Jackson GS, Enke CG: Effects of salt concentration on analyte response using electrospray ionization mass spectrometry. *J Am Soc Mass Spectrom* 1999, **10**:625-634.

15. Makawita S, Diamandis EP: The bottleneck in the cancer biomarker pipeline and protein quantification through mass spectrometry-based approaches: current strategies for candidate verification. *Clin Chem* 2010, **56**:212-222.
16. Hattan SJ, Parker KC: Methodology utilizing MS signal intensity and LC retention time for quantitative analysis and precursor ion selection in proteomic LC-MALDI analyses. *Anal Chem* 2006, **78**:7986-7996.
17. Sahu A, Lambris JD: Structure and biology of complement protein C3, a connecting link between innate and acquired immunity. *Immunol Rev* 2001, **180**:35-48.
18. Lochnit G, Geyer R: An optimized protocol for nano-LC-MALDI-TOF-MS coupling for the analysis of proteolytic digests of glycoproteins. *Biomed Chromatogr* 2004, **18**:841-848.
19. Wuhler M, Catalina MI, Deelder AM, Hokke CH: Glycoproteomics based on tandem mass spectrometry of glycopeptides. *J Chromatogr B Analyt Technol Biomed Life Sci* 2007, **849**:115-128.
20. Liu T, Qian WJ, Gritsenko MA, Xiao W, Moldawer LL, Kaushal A, Monroe ME, Varnum SM, Moore RJ, Purvine SO, et al: High dynamic range characterization of the trauma patient plasma proteome. *Mol Cell Proteomics* 2006, **5**:1899-1913.
21. Wang Y, Wu SL, Hancock WS: Approaches to the study of N-linked glycoproteins in human plasma using lectin affinity chromatography and nano-HPLC coupled to electrospray linear ion trap-Fourier transform mass spectrometry. *Glycobiology* 2006, **16**:514-523.
22. Angel PM, Lim JM, Wells L, Bergmann C, Orlando R: A potential pitfall in 18O-based N-linked glycosylation site mapping. *Rapid Commun Mass Spectrom* 2007, **21**:674-682.
23. Fukuyama Y, Nakaya S, Yamazaki Y, Tanaka K: Ionic liquid matrixes optimized for MALDI-MS of sulfated/sialylated/neutral oligosaccharides and glycopeptides. *Anal Chem* 2008, **80**:2171-2179.
24. Seraglia R, Molin L, Tonidandel L, Pucciarelli S, Agostini M, Urso ED, Bedin C, Quaia M, Nitti D, Traldi P: An investigation on the nature of the peptide at m/z 904, overexpressed in plasma of patients with colorectal cancer and familial adenomatous polyposis. *J Mass Spectrom* 2007, **42**:1606-1612.
25. Xue H, Lu B, Zhang J, Wu M, Huang Q, Wu Q, Sheng H, Wu D, Hu J, Lai M: Identification of serum biomarkers for colorectal cancer metastasis using a differential secretome approach. *J Proteome Res* 2010, **9**:545-555.
26. Huber R, Scholze H, Paques EP, Deisenhofer J: Crystal structure analysis and molecular model of human C3a anaphylatoxin. *Hoppe Seylers Z Physiol Chem* 1980, **361**:1389-1399.
27. Ward DG, Suggett N, Cheng Y, Wei W, Johnson H, Billingham LJ, Ismail T, Wakelam MJ, Johnson PJ, Martin A: Identification of serum biomarkers for colon cancer by proteomic analysis. *Br J Cancer* 2006, **94**:1898-1905.
28. Lee IN, Chen CH, Sheu JC, Lee HS, Huang GT, Chen DS, Yu CY, Wen CL, Lu FJ, Chow LP: Identification of complement C3a as a candidate biomarker in human chronic hepatitis C and HCV-related hepatocellular carcinoma using a proteomics approach. *Proteomics* 2006, **6**:2865-2873.
29. Zhang R, Barker L, Pinchev D, Marshall J, Rasamoeliso M, Smith C, Kupchak P, Kireeva I, Ingratta L, Jackowski G: Mining biomarkers in human sera using proteomic tools. *Proteomics* 2004, **4**:244-256.
30. Miguet L, Bogumil R, Decloquement P, Herbrecht R, Potier N, Mauvieux L, Van Dorsselaer A: Discovery and identification of potential biomarkers in a prospective study of chronic lymphoid malignancies using SELDI-TOF-MS. *J Proteome Res* 2006, **5**:2258-2269.
31. Diefenbach RJ, Isenman DE: Mutation of residues in the C3dg region of human complement component C3 corresponding to a proposed binding site for complement receptor type 2 (CR2, CD21) does not abolish binding of iC3b or C3dg to CR2. *J Immunol* 1995, **154**:2303-2320.
32. Lu P, Vogel C, Wang R, Yao X, Marcotte EM: Absolute protein expression profiling estimates the relative contributions of transcriptional and translational regulation. *Nat Biotechnol* 2007, **25**:117-124.
33. Ishihama Y, Oda Y, Tabata T, Sato T, Nagasu T, Rappsilber J, Mann M: Exponentially modified protein abundance index (emPAI) for estimation of absolute protein amount in proteomics by the number of sequenced peptides per protein. *Mol Cell Proteomics* 2005, **4**:1265-1272.
34. Rower C, Vissers JP, Koy C, Kipping M, Hecker M, Reimer T, Gerber B, Thiesen HJ, Glocker MQ: Towards a proteome signature for invasive ductal breast carcinoma derived from label-free nanoscale LC-MS protein expression profiling of tumorous and glandular tissue. *Anal Bioanal Chem* 2009, **395**:2443-2456.
35. Monroe ME, Tolic N, Jaitly N, Shaw JL, Adkins JN, Smith RD: VIPER: an advanced software package to support high-throughput LC-MS peptide identification. *Bioinformatics* 2007, **23**:2021-2023.
36. Washburn MP, Wolters D, Yates JR: Large-scale analysis of the yeast proteome by multidimensional protein identification technology. *Nat Biotechnol* 2001, **19**:242-247.
37. Wu CC, MacCoss MJ, Howell KE, Yates JR: A method for the comprehensive proteomic analysis of membrane proteins. *Nat Biotechnol* 2003, **21**:532-538.
38. Iwasaki M, Miwa S, Ikegami T, Tomita M, Tanaka N, Ishihama Y: One-dimensional capillary liquid chromatographic separation coupled with tandem mass spectrometry unveils the *Escherichia coli* proteome on a microarray scale. *Anal Chem* 2010, **82**:2616-2620.
39. Knochenmuss R, Zenobi R: MALDI ionization: the role of in-plume processes. *Chem Rev* 2003, **103**:441-452.

doi:10.1186/1477-5956-9-18

Cite this article as: Toyama et al.: Deglycosylation and label-free quantitative LC-MALDI MS applied to efficient serum biomarker discovery of lung cancer. *Proteome Science* 2011 **9**:18.

Submit your next manuscript to BioMed Central and take full advantage of:

- Convenient online submission
- Thorough peer review
- No space constraints or color figure charges
- Immediate publication on acceptance
- Inclusion in PubMed, CAS, Scopus and Google Scholar
- Research which is freely available for redistribution

Submit your manuscript at
www.biomedcentral.com/submit



A Comprehensive Peptidome Profiling Technology for the Identification of Early Detection Biomarkers for Lung Adenocarcinoma

Koji Ueda^{1*}, Naomi Saichi¹, Sachiko Takami², Daechun Kang^{1,3}, Atsuhiko Toyama^{1,3,4}, Yataro Daigo³, Nobuhisa Ishikawa⁵, Nobuoki Kohno⁵, Kenji Tamura⁶, Taro Shuin⁶, Masato Nakayama⁷, Taka-Aki Sato⁴, Yusuke Nakamura³, Hidewaki Nakagawa^{1*}

1 Laboratory for Biomarker Development, Center for Genomic Medicine, RIKEN, Yokohama, Japan, **2** CSK Institute for Sustainability, Ltd., Tokyo, Japan, **3** Laboratory of Molecular Medicine, Human Genome Center, Institute of Medical Science, The University of Tokyo, Tokyo, Japan, **4** Shimadzu Corporation, Kyoto, Japan, **5** Department of Molecular and Internal Medicine, Hiroshima University, Hiroshima, Japan, **6** Department of Urology, Kochi University School of Medicine, Nankoku, Japan, **7** Toppan Printing Co., Ltd., Tokyo, Japan

Abstract

The mass spectrometry-based peptidomics approaches have proven its usefulness in several areas such as the discovery of physiologically active peptides or biomarker candidates derived from various biological fluids including blood and cerebrospinal fluid. However, to identify biomarkers that are reproducible and clinically applicable, development of a novel technology, which enables rapid, sensitive, and quantitative analysis using hundreds of clinical specimens, has been eagerly awaited. Here we report an integrative peptidomic approach for identification of lung cancer-specific serum peptide biomarkers. It is based on the one-step effective enrichment of peptidome fractions (molecular weight of 1,000–5,000) with size exclusion chromatography in combination with the precise label-free quantification analysis of nano-LC/MS/MS data set using Expressionist proteome server platform. We applied this method to 92 serum samples well-managed with our SOP (standard operating procedure) (30 healthy controls and 62 lung adenocarcinoma patients), and quantitatively assessed the detected 3,537 peptide signals. Among them, 118 peptides showed significantly altered serum levels between the control and lung cancer groups ($p < 0.01$ and fold change > 5.0). Subsequently we identified peptide sequences by MS/MS analysis and further assessed the reproducibility of Expressionist-based quantification results and their diagnostic powers by MRM-based relative-quantification analysis for 96 independently prepared serum samples and found that APOA4 273–283, FIBA 5–16, and LBN 306–313 should be clinically useful biomarkers for both early detection and tumor staging of lung cancer. Our peptidome profiling technology can provide simple, high-throughput, and reliable quantification of a large number of clinical samples, which is applicable for diverse peptidome-targeting biomarker discoveries using any types of biological specimens.

Citation: Ueda K, Saichi N, Takami S, Kang D, Toyama A, et al. (2011) A Comprehensive Peptidome Profiling Technology for the Identification of Early Detection Biomarkers for Lung Adenocarcinoma. PLoS ONE 6(4): e18567. doi:10.1371/journal.pone.0018567

Editor: Richard C. Willson, University of Houston, United States of America

Received: November 16, 2010; **Accepted:** March 4, 2011; **Published:** April 12, 2011

Copyright: © 2011 Ueda et al. This is an open-access article distributed under the terms of the Creative Commons Attribution License, which permits unrestricted use, distribution, and reproduction in any medium, provided the original author and source are credited.

Funding: This study was supported by Japanese Ministry of Education, Culture, Sports, Science and Technology (Wakate-A, 22680064, <http://kaken.nii.ac.jp/ja/p/22680064>). This study was also funded by Shimadzu Corporation, CSK Institute for Sustainability, Ltd., Toppan Printing Co., Ltd. As employers of ST, AT, TS, or MN in this study, these funders did play a role in the study design, data collection and analysis, decision to publish, or preparation of the manuscript.

Competing Interests: ST is an employee of CSK Institute for Sustainability, Ltd. AT and TS are employees of Shimadzu Corporation. MN is an employee of Toppan Printing Co., Ltd. They contributed to the technical support and data analysis of this manuscript. The companies listed above also funded for this study, since this collaborative work was performed in "the academic-industrial alliance project for the development of lung cancer early detection system" among RIKEN, the University of Tokyo, Shimadzu Corporation, Toppan Printing Co., Ltd., and CSK Institute for Sustainability, Ltd. This does not alter the authors' adherence to all the PLoS ONE policies on sharing data and materials.

* E-mail: k-ueda@riken.jp (KU); hidewaki@ims.u-tokyo.ac.jp (HN)

Introduction

Lung cancer is the leading cause of cancer death worldwide [1]. Smoking is still the leading risk factor for lung cancer, but recently the proportion of never smoker-related lung cancer is significantly increasing, although its cause or other risk factor(s) is unknown [2]. Lung cancer patients show the poor prognosis with an overall 5-year survival rate of only 15% [3]. One of the reasons for this dismal prognosis is no effective tools to detect it at an early stage and in fact only 16% of patients are diagnosed at their early stage of the disease [3]. Current screening methods such as chest X-ray or cytological examination of sputum have not yet shown their effectiveness in the improvement of mortality of lung cancer,

whereas low dose helical CT have been proved to possess a potential to detect early-stage lung cancer and demonstrate 20% lower lung cancer mortality rate compared to chest X-ray screening [4]. On the other hand, serum biomarkers for lung cancer have been investigated to achieve early detection of the disease and improve clinical management of patients [5]. Nonetheless, their present clinical usefulness remains limited [6,7]. CEA (carcinoembryonic antigen) and CYFRA (cytokeratin 19 fragment) are elevated in sera in a subset of lung cancer patients, and are clinically applied to monitor the disease status and evaluate the response to treatments. However, they are not recommended to use in clinical diagnosis and screening [8] because they are also elevated in certain non-cancerous conditions

such as smoking and lung inflammation as well as in patients with other types of cancers. It is obvious that CEA and CYFRA do not have the sufficient power to apply for the screening of early-stage lung cancer. Hence, development of novel serum/plasma biomarkers applicable for lung cancer diagnosis is urgently required.

Recently monitoring the protein expression pattern in clinical specimens by proteomics technologies has offered great opportunities to discover potentially new biomarkers for cancer diagnosis. Various proteomic tools such as 2D-DIGE, SELDI-TOF-MS, protein arrays, ICA1, iTRAQ and MudPIT have been used for differential analysis of biological samples including cell lysates and blood to better understand the molecular basis of cancer pathogenesis and the characterization of disease-associated proteins [9]. In order to explore putative biomarkers in complicated biological samples, focused proteomics or targeted proteomics technologies have been utilized such as; phosphoprotein enrichment technologies IMAC [10], the cell-surface-capturing (CSC) technology [11,12], glycan structure-specific quantification technology IGEL [13]. Most recently, to identify novel lung cancer biomarkers, Ostroff *et al.* reported the aptamer-based proteomic technology targeting 813 known proteins. Finally they selected 12 proteins which discriminated NSCLC from controls with 89% sensitivity and 83% specificity [14]. Thus targeted proteomics technologies such as the aptamer method would be applicable for the measurement of already known proteins, however could not be applied for the discovery of biomarkers targeting unknown proteins, post translational modifications, or biologically-processed polypeptides.

These methods can circumvent the technological limitations that currently prohibit the sensitive and high-throughput profiling of, in particular, blood proteome samples because of its high complexity and large dynamic range of proteins. The peptidome profiling technology addressed in the present study is one of the focused proteomics approaches targeting on biosynthetic fragments of proteins/peptides in blood, involving bioactive peptides and those non-specifically degraded by proteases or peptidases [15,16].

So far more than 500 proteases/peptidases are known to be expressed in human cells [17,18]. They function at almost all locations in the body including intracellular region, extracellular matrices, and in blood, involved in activation of other protein functions, degradation of cellular proteins, and notably tumor progression or suppression [19,20,21]. Indeed many matrix metalloproteases are overexpressed in various types of tumor cells, that facilitate construction of favorable micro-environment for tumor cells or promotion of metastasis [21]. Definitely these protease/peptidase activities should result in the production of digested peptide fragments well reflecting the tumor progression or tumor-associated responses. Thus peptidomic profiling of human serum or plasma is a promising tool for the discovery of novel tumor markers.

In this article, we extracted peptidome fractions (molecular weight <5,000 Da) from 92 individuals using the well-established and reproducible one-step peptidome enrichment method based on size exclusion chromatography (SEC) [22,23] and provided them to the label-free mass spectrometric quantification analysis combined with the statistical analyses on Expressionist proteome server platform. Our rapid and simple peptidome enrichment procedure can circumvent both less reproducible peptidome extraction by such as ultrafiltration spin filters and prolonged sample preparation including immuno-depletion column chromatography, denaturing proteins, buffer exchange, ultrafiltration, and so on [16]. After quantitative comparison of 3,537 serum peptides

among 92 cases in the lung cancer biomarker discovery, we further evaluated the accuracy of quantification results by another more reliable quantification method MRM (multiple reaction monitoring) technology using independently prepared 96 serum samples.

Materials and Methods

Serum samples

All human serum samples were obtained with informed consent from 122 patients with lung adenocarcinoma (stage I to IV) at Hiroshima University Hospital at the examination on admission. Serum samples as normal controls were also obtained with informed consent from 30 healthy volunteers who received medical checkup at Hiroshima NTT Hospital and 36 from Kochi University Hospital. Each consent above was given in writing. To circumvent undesirable degradation of proteins and peptides, all serum samples were collected and stored under unified SOP. Briefly, all venous blood specimens were collected with vacuum blood collection tubes TERUMO VP-P070K (TERUMO, Tokyo, Japan). After staying upright at ambient temperature for 60 minutes, serum fractions were separated with centrifugation at 1500 × *g* for 15 min (4°C) and immediately stored at -80 °C. One freeze-and-thaw procedure was permitted for any serum samples used in the present study. This study was approved by individual institutional ethical committees; The Ethical Committee of Yokohama Institute, RIKEN (Approval code: Yokohama H20-12), The Ethical Committee of Hiroshima University Hospital, and The Ethical Committee of Kochi University Hospital.

Heat inactivation of sera and subsequent peptidome enrichment

All serum samples were frozen and thawed once and immediately incubated at 100 °C for 10 minutes after 4 times dilution with proteomics grade water. Following filtration with Spin-X 0.45 μm spin filters (Corning Incorporated, Corning, NY, USA), samples were loaded into 10/300 Superdex peptide column (GE Healthcare UK Ltd., Buckinghamshire, England) coupled with Prominence HPLC system (Shimadzu Corporation, Kyoto, Japan). The peptidome fraction was collected from 22 to 34 minutes in the constant flow of 100 mM ammonium acetate at 0.5 ml/min flow rate. The collected fractions were dried-up with Vacuum Spin Drier (TAITEC Co., Ltd., Saitama, Japan).

LC/MS/MS analysis for the screening study

The dried peptide samples were resuspended in 2% acetonitrile with 0.1% trifluoroacetic acid and analyzed by QSTAR-Elite mass spectrometer (AB Sciex, Foster City, CA, USA) combined with UltiMate 3000 nano-flow HPLC system (DIONEX Corporation, Sunnyvale, CA, USA). Samples were separated on the 100 μm × 200 mm tip-column (GL Sciences Inc., Tokyo, Japan), in which L-Column beads (Chemicals Evaluation and Research Institute, Tokyo, Japan) were manually loaded, using solvent A [0.1% formic acid, 2% acetonitrile] and solvent B [0.1% formic acid, 70% acetonitrile] with the multistep linear gradient of solvent B 5 to 55% for 95 minutes and 55 to 95% for 10 minutes at a flow rate 200 nl/min. The elute was directly analyzed with the 1 second MS survey (*m/z* 400 1800) followed by three MS/MS measurements on the most intense parent ions (30 counts threshold, +2 - +4 charge state, and *m/z* range 50 2000), using the "smart exit" setting (SIDA = 3.0, max accumulation time = 2.0 sec.). Previously targeted parent ions were excluded from repetitive MS/MS acquisition for 40 seconds (100 mDa mass tolerance). The other parameters on QSTAR-Elite were shown as follows: DP = 60, FP = 265, DP2 = 15, CAD = 5, IRD = 6,

IRW = 5, Curtain gas = 20, and Ion spray voltage = 1600 V. The mass of each run was calibrated using three typical polysiloxane-derived background peaks: m/z = 445.12003, 519.13882, and 667.17640. The resolution of mass spectra was around 20,000 at m/z = 400. The primary data files (formatted as wiff and wiff.scan) from 92 clinical samples are available in a public repository site Proteome Commons (<https://proteomecommons.org/>). The MASCOT database search was performed on the Analyst QS 2.0 software (AB Sciex, Foster City, CA, USA). The MS/MS data was searched against the human protein database from SwissProt 57.4 (20,400 sequences) using the search parameters: Taxonomy = Homo sapiens, Enzyme = None, Fixed modifications = None, Variable modifications = Oxidation (Met), MS tolerance = 50 ppm, and MS/MS tolerance = 0.1 Da, with Mascot Automatic Decoy Search. Although Matrix Science recommends to use the Homology threshold for less-stringent criteria or Identity threshold providing almost same protein identification numbers with the criteria Expectation value < 0.05 (http://www.matrixscience.com/help/interpretation_help.html), we accepted peptide identifications that satisfied both the false discovery rate (FDR) of peptide matches above identity threshold less than 5% and the Expectation value < 0.05 in order to obtain more reliable identification of individual peptides than that from Mascot default criteria.

Alignment of MS chromatogram planes and peak detection on Expressionist RefinerMS

The raw data files from QSTAR-Elite (.wiff and wiff.scan formatted) were directly loaded onto the Genedata Expressionist modules (Genedata AG, Basel, Switzerland). Genedata Expressionist worked on the in-house server system HP-DL380-G5 (Hewlett-Packard Development Company, Palo Alto, CA, USA) equipped with 16 GB memory, (72 GB×2) + (146 GB×25) RAID 0+1 hard disks, and SUSE Linux Enterprise Server 10 SP2 operating system, installed with Oracle 10 g ver. 10.2.0.4. software (Oracle Corporation, Redwood Shores, CA, USA). All MS chromatograms were smoothed with RT Window = 3 scans in the Chromatogram Chemical Noise Subtraction Activity. To remove the background noise, a peak intensity is defined as follows.

$$\text{Intensity}_{\text{subtracted}} = \max(\text{Intensity}_{\text{original}} - \text{Quantile} - \text{Threshold}, 0)$$

Here, values Quantile = 50%, Intensity Threshold = 15 cps were used. Furthermore signals satisfying at least one of the following criteria were considered as noise peaks and subtracted: RT Window > 50 scans, Minimum RT Length = 4 scans, or Minimum m/z Length = 8 data points. Then MS chromatogram planes derived from 92 serum samples were accurately aligned using parameters: m/z Window = 0.1 Da, RT Window = 0.2 min, Gap Penalty = 1, and RT Search Interval = 5 min in the Chromatogram RT Alignment Activity. Next, the Summed Peak Detection Activity detected the peaks on a temporary averaged chromatogram with parameters as follows: Summation Window = 5 scans, Overlap = 50, Minimum Peak Size = 4 scans, Maximum Merge Distance = 10 data points, Gap/Peak Ratio = 1, Method = curvature-based peak detection, Peak Refinement Threshold = 5, Consistency Filter Threshold = 0.8, Signal/Noise Threshold = 1. Finally the two steps Summed Isotope Clustering Activity identified isotope patterns among 2D peaks, in which peaks identified as belonging to the same isotope pattern of a molecule were grouped into peak clusters. The first clustering was performed with the

following criteria: Minimum Charge = 1, Maximum Charge = 10, Maximum Missing Peaks = 0, First Allowed Gap Position = 3, Ionization = protonation, RT Tolerance = 0.1 min, m/z Tolerance = 0.05 Da, Isotope Shape Tolerance = 10.0, and Minimum Cluster Size Ratio = 1.2. The second clustering was performed with the same setting above, except for Minimum Cluster Size Ratio = 0.6 and Reuse Existing Clusters = true. The information of all detected cluster peaks, including m/z , retention time, and intensity, was exported as ABS files.

Label-free quantification and statistical analysis on Expressionist Analyst

The ABS files were loaded on the Expressionist Analyst module (Genedata AG, Basel, Switzerland). The peak intensity variation among 32 samples was normalized by fixing the median intensity of each sample at 10,000. Using the normalized intensity data, Student's t-test was performed between the normal group ($n = 30$) and lung cancer patients group ($n = 62$). The candidate biomarker peaks were extracted which showed $p < 0.01$ and fold-change > 5.0 between two groups. The candidates were further selected by Absent/Present Search to identify peaks with all-or-nothing detection pattern, which were detectable in 15 or all of 16 samples in one group and 1 or none of 16 samples in another group.

Multiple Reaction Monitoring

Serum samples were processed with Superdex peptide column chromatography as described above before mass spectrometric analyses. The dried peptide samples were resuspended with 1 fmol/ μ l BSA tryptic digest solution in 2% acetonitrile, 0.1% trifluoroacetic acid and analyzed by 4000 QTRAP mass spectrometer (AB Sciex, Foster City, CA, USA) combined with Paradigm MS4 PAL nano-flow HPLC system (AMR Inc., Tokyo, Japan). Peptides were separated on the 100 μ m×100 mm tip-column (GL Sciences Inc., Tokyo, Japan), in which L-Column ODS beads (Chemicals Evaluation and Research Institute, Saitama, Japan) were manually loaded. Using solvent A [0.1% formic acid, 2% acetonitrile] and solvent B [0.1% formic acid, 90% acetonitrile], the linear gradient of solvent B 2 to 100% for 10 minutes was configured at a flow rate 200 nl/min. 19 targeted peptide ions and 5 BSA-derived peptide ions were simultaneously monitored by the MRM mode in Analyst 1.5 software (AB Sciex, Foster City, CA, USA) in duplicate. The MRM transitions are shown in **Table S4**. The acquired MRM chromatograms were then smoothed and quantified with MultiQuant software (AB Sciex, Foster City, CA, USA). MRM peak areas in each sample were normalized as follows:

$$\text{Area}_{\text{Normalized}} = \frac{\text{Area}_{\text{Raw data}}}{(\text{summed area of 5 BSA standards}) \times 1000}$$

Box plot analysis and ROC curve analysis

The averaged area of the duplicated MRM chromatogram peak corresponding to 19 candidate biomarker peptides was used to create box plot with R algorithm. For each study the box represents the middle half of the distribution of the data points stretching from the 25th percentile to the 75th percentile. The line across the box represents the median. The lengths of the lines above and below the box are defined by the maximum and minimum datapoint values, respectively, that lie within 1.5 times the spread of the box. Results of Student's t-test were included on the box plot. ROC curves were also depicted by R. The cut-off value was set at the point whose

distance from the (sensitivity, specificity) = (1, 1) reached the minimum. The sensitivity (Sens), specificity (Spec), positive predictive value (PV+), negative predictive value (PV-), and area under the curve (AUC) were shown on each graph.

Results

The efficient enrichment of peptidome fractions from sera

Since reproducible and accurate separation of the peptidome fraction from serum was essential for the effective screening of biomarkers, we optimized a simple gel filtration chromatography method (Fig. 1) and evaluated the peptide recovery. To avoid uncontrolled degradation of serum components arising from intact proteases and peptidases, all serum samples were immediately heated at 100 °C for 10 min after only one freeze-thaw procedure. Four-fold dilution of serum with water could eliminate the protein aggregation during heat inactivation even though the samples appeared slightly

cloudy. Figure 2A shows the merged gel filtration HPLC chromatograms from 16 individual serum samples using the Superdex Peptide 10/300 column. The spectra illustrated highly reproducible separation of serum proteins and peptides. Then, the accuracy of size exclusion chromatography was assessed by analyzing 10 fractions (2 min each from retention time for the period of 14–34 min, Fig. 2B) with the MALDI-TOF-TOF mass spectrometer (Fig. 2C). As shown by the continuous MS spectra in Figure 2C, our gel filtration chromatography procedure allowed precise separation of serum proteins and peptides based on their molecular weights. Consequently we defined the fraction numbers 5 to 10 (corresponding to molecular weight 1,000 to 5,000) that should be focused in the further biomarker screening and validation studies.

Label-free quantification-based peptide biomarker screening for lung cancer

To explore serum peptides which could be applied for early detection of lung cancer, we acquired quantitative peptidome

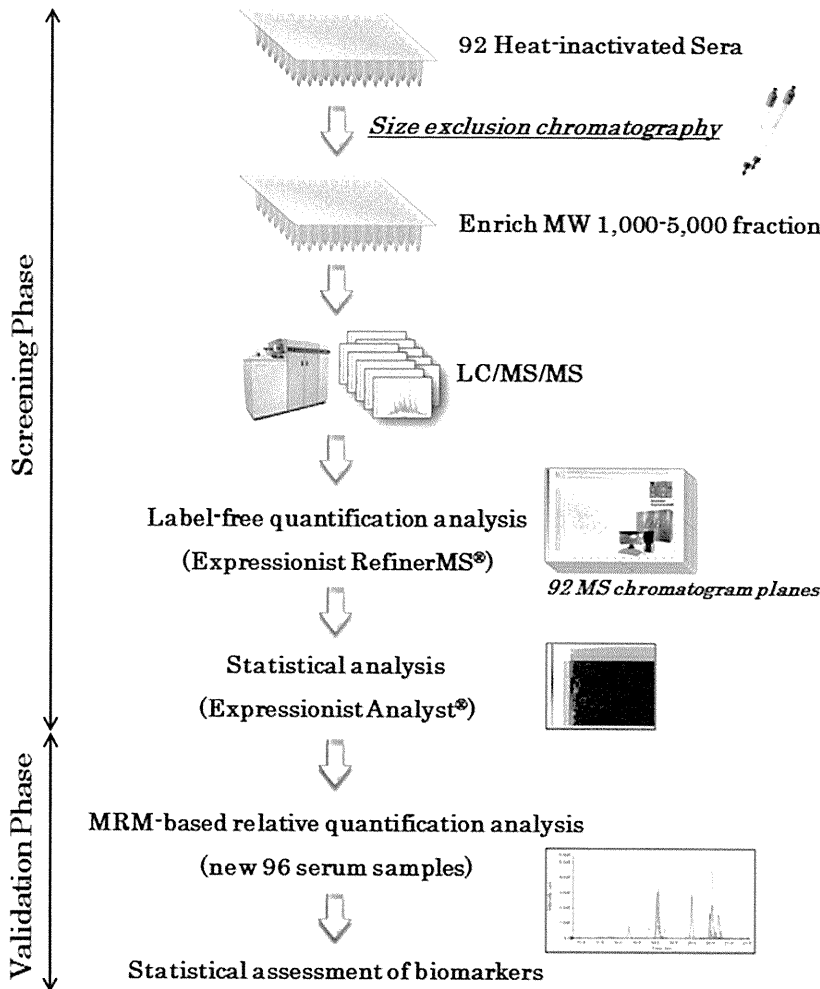


Figure 1. Schematic view of peptidome biomarker development workflow. In the screening phase, 92 serum samples were initially heat inactivated. The peptidome fractions enriched with gel filtration chromatography were analyzed with QSTAR-Elite LC/MS/MS. Following LC/MS data processing and label-free quantification analysis on the Expressionist RefinerMS module, candidate biomarkers were statistically extracted by the Expressionist Analyst module. In the validation phase, MRM experiments were performed to assess the applicability of 19 biomarker candidates using additional 96 serum samples.

doi:10.1371/journal.pone.0018567.g001

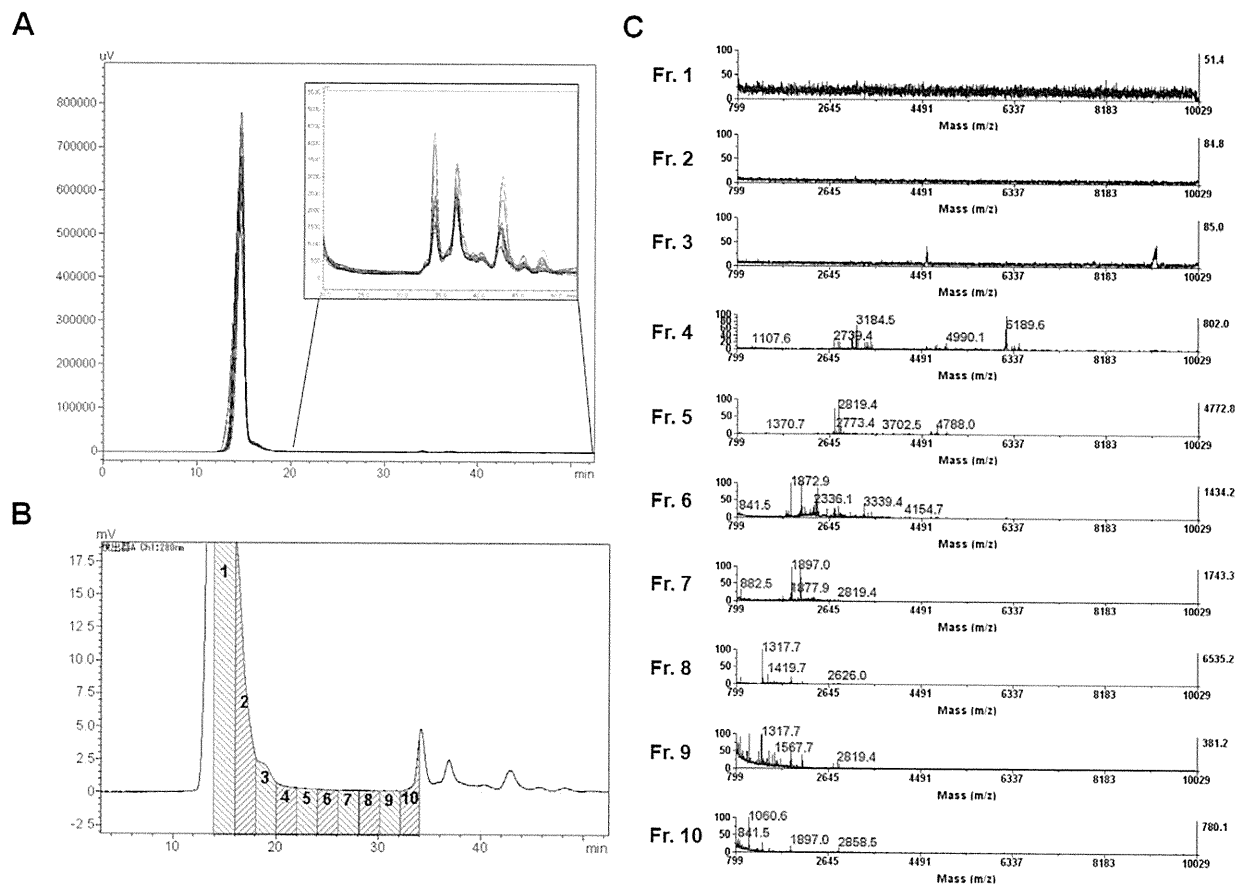


Figure 2. Simple and efficient enrichment of serum peptidome fractions by gel filtration chromatography. (A) The merged display of 16 independent spectra of gel filtration chromatography (280 nm UV absorbance). 10 μ l each of serum sample was loaded. The upper right box shows the magnified view of the retention time range from 20 to 50 minutes. (B)(C) To evaluate the fractionation efficacy of Superdex Peptide 10/300 column, the elute was separated into 10 fractions and analyzed with MALDI-TOF mass spectrometer. The numbers of fractions in B correspond to the spectra numbers in C. doi:10.1371/journal.pone.0018567.g002

profiles from 92 individuals (**Table S1**) including 62 lung cancer patients that consisted of 32 patients with an operable lung cancer (stage-I: $n = 10$, stage-II: $n = 10$, stage-IIIa: $n = 12$) and 30 lung cancer patients at an advanced stage (stage-IIIb: $n = 15$, stage-IV: $n = 15$) to identify candidate serum biomarkers for lung cancer. The serum samples were purified using gel filtration chromatography as described above and individually subjected to LC/MS/MS analyses using QSTAR-Elite mass spectrometer (Fig. 1). Subsequently 92 MS raw data were loaded and processed on the Expressionist RefinerMS module (Fig. 3A). Genedata Expressionist is an enterprise system for omics data management comprised of integrated software modules, which support the complete R&D processes involving data processing, statistical analysis, data management and result reporting. The technology-dependent modules for microarray data (Refiner Array), mass spectrometry (Refiner MS, used in the present study) and genomic profiling (Refiner Genome) allow highly-sophisticated data processing, quantification, visualization, and result exporting in any generally-used formats. Once all data are quantified and summarized, they can be seamlessly analyzed with the Genedata Analyst module employing various statistical analyses. This system initially made the MS chromatogram planes as shown in Figure 3C, and subtracted the instrument specific noises and chemical noises

effectively. At the fourth step of the workflow in Figure 3A, the retention time (RT) grids on each MS chromatogram plane were perfectly aligned among these 92 samples (Fig. 3B), which allowed the solid quantification analysis of multiple samples. Subsequently, peaks were detected from temporarily averaged m/z -RT planes by the Chromatogram Summed Peak Detection Activity in order to avoid missing peak-location information even if the peaks were not detectable in particular planes. The detected isotopic peaks belonging to the same peptide signals were grouped into individual clusters that are displayed as colored rectangles in Figure 3C. A total of 12,396 non-redundant isotopic peak clusters with charge state +1 to +10 were detected from 92 serum samples. We then utilized 3,537 clusters with charge stage +2 to +10 for further statistical considerations in the Expressionist Analyst module, since singly-charged ions might include substantial proportion of non-peptide components such as chemicals.

Student's t-test was applied to investigate the differences in their serum levels between the normal group ($n = 30$) and the lung cancer group ($n = 62$) (Fig. 4A). This analysis identified 118 candidate biomarker peptides ($p < 0.01$ and fold-change of > 5.0). Since the criteria of t-test were variable for the purpose of candidate selection, we used the threshold above just in order to define the highest priority group. The intensity distributions of these peptides were

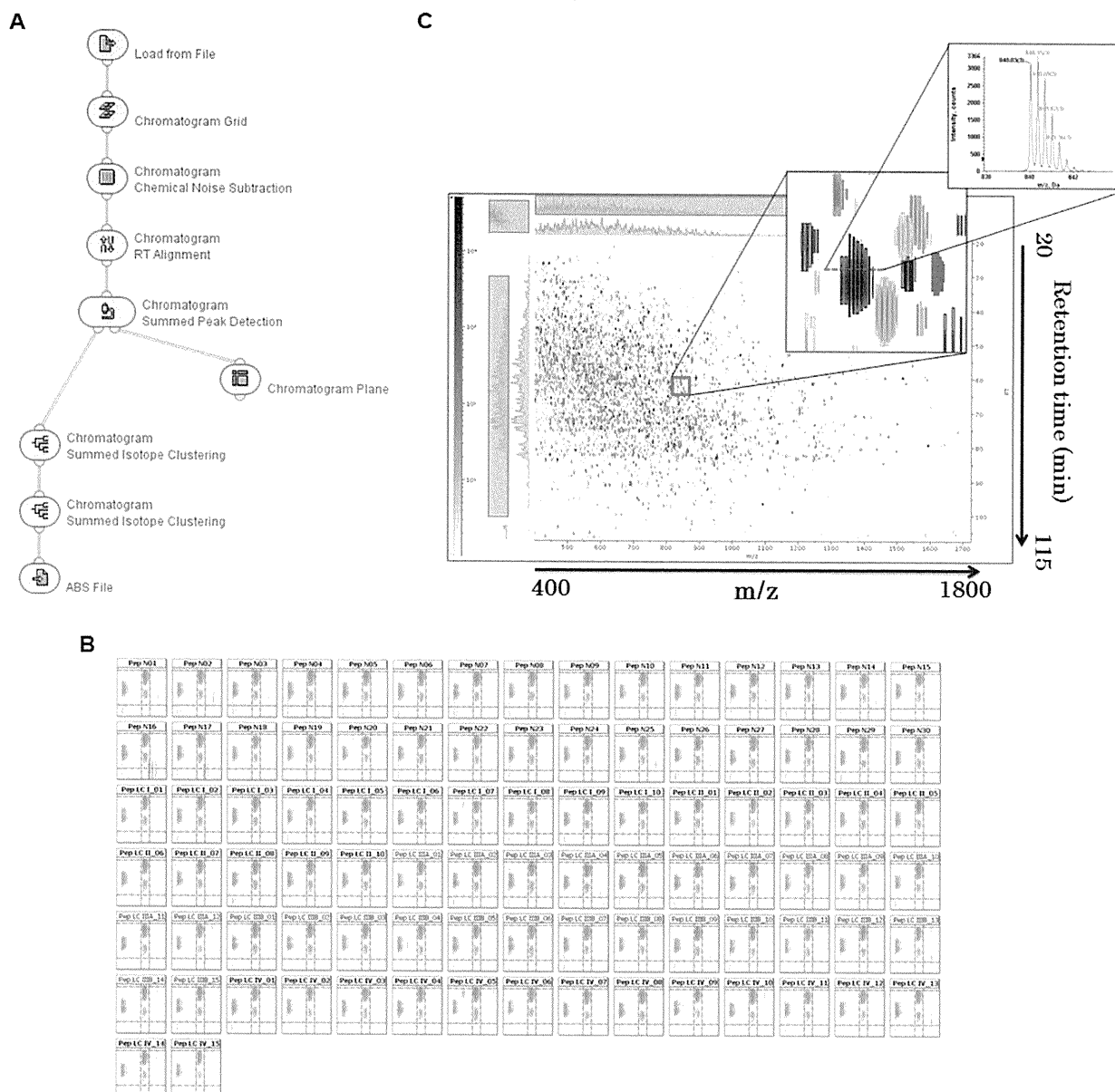


Figure 3. Rapid and accurate data processing for label-free quantification on the Expressionist RefinerMS module. (A) The total workflow used in the Expressionist RefinerMS module. Only 3 hours were needed to complete entire steps in this workflow on 92 LC/MS/MS data (each with 120 minutes LC gradient). (B) The representative area of m/z - retention time planes after RT alignment of 92 LC/MS/MS data. In each panel, three isotopic clusters and grid lines were displayed, showing highly exact alignments. (C) The MS chromatogram plane in which all data processing were completed. Finally, isotopic clusters derived from a single peptide were grouped into a colored cluster as shown in the middle panel. The far right panel shows the MS spectrum corresponding to the horizontal section view of a representative cluster. doi:10.1371/journal.pone.0018567.g003

visualized with bar charts in Figure S1. The subsequent principal component analysis demonstrated that the values of 118 candidate biomarker peptides could explicitly separate control and lung cancer groups on the 3D plot using principal component 1, 2, and 3 (Fig. 4B). The proportion of variance described by the principal component 1, 2, or 3 was 66.9%, 15.0%, or 4.4%, respectively, indicating that illustrated components 1 to 3 could reflect 86.3% (the cumulative proportion) of quantitative information in this mass spectrometric screening analysis.

Identification of peptide sequences by LC/MS/MS

Alongside the label-free quantification-based biomarker screening described above, the comprehensive peptide sequencing was performed by a combination of QSTAR-Elite LC/MS/MS analysis and MASCOT database search. Among 230,657 MS/MS queries from 92 serum samples, 5,382 peptides were successfully sequenced with MASCOT expectation value <0.05 (FDR of peptide matches above Identity threshold was 1.49%). After examining redundancy, 424 unique peptides were

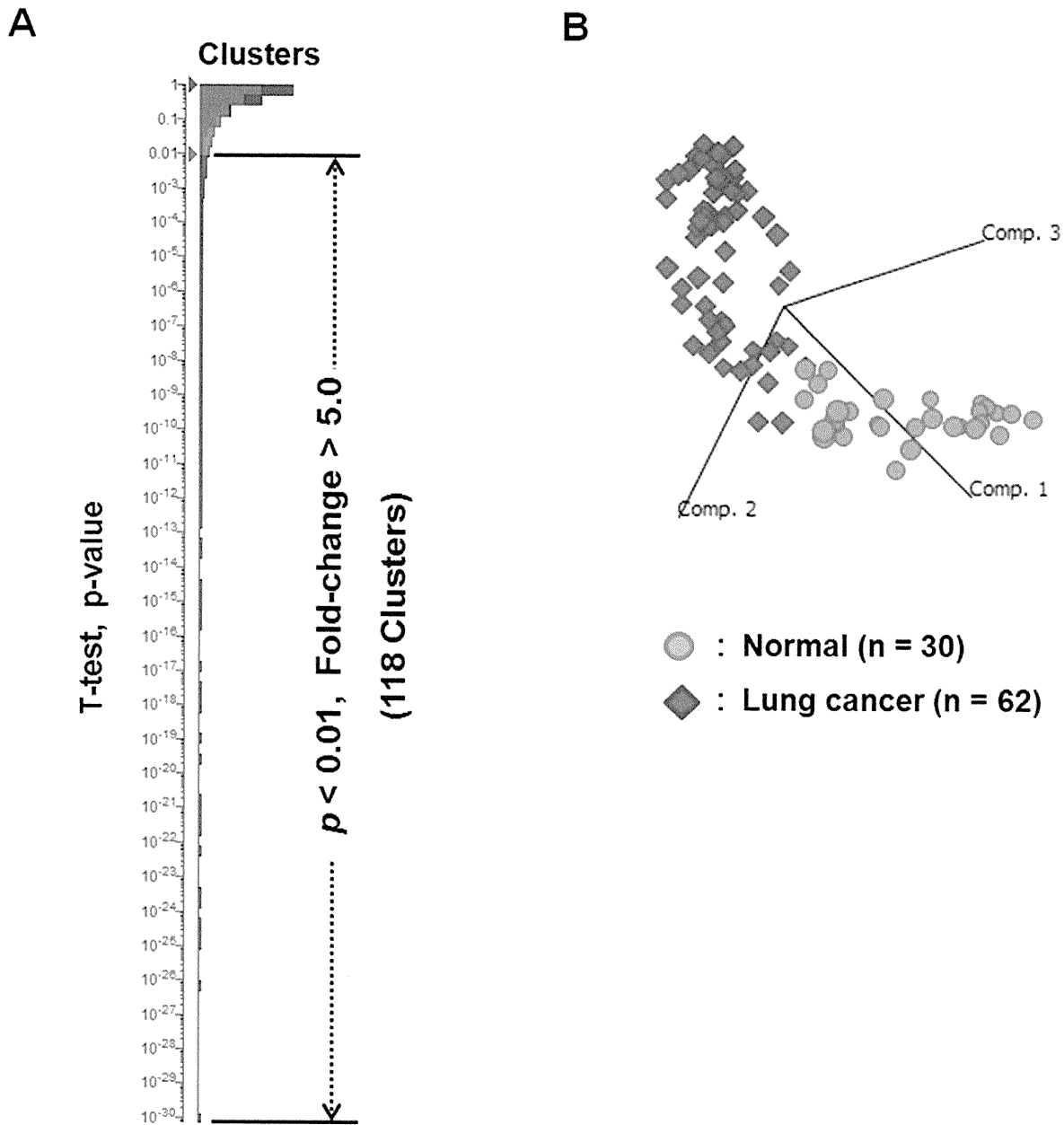


Figure 4. Statistical identification of candidate biomarkers for lung cancer. (A) The hierarchy chart of clusters (peptides) according to Student's t-test p-values (normal group vs. lung cancer group). 118 peptides satisfied the criteria of $p < 0.01$ and fold change > 5.0 . (B) Principal component analysis using the values of 118 candidate biomarker peptides showed clear separation between control and lung cancer groups on the 3D plot. The proportion of variance described by the principal component 1, 2, or 3 was 66.9%, 15.0%, or 4.4%, respectively.
doi:10.1371/journal.pone.0018567.g004

identified that corresponded to 106 proteins (**Table S2**). Regarding the 118 candidate peptides, 19 peptides were uniquely identified; 12 of them were found to be derivatives from fibrinogen alpha chain (FIBA), 4 from apolipoprotein A-IV (APOA4), and the remaining three peptides were turned out to be a fragment of amiloride-sensitive cation channel 4 (ACCN4), apolipoprotein E (APOE), and limbin (LBN) (**Table 1**).

MRM-based validation experiment for 19 candidate biomarker peptides

To assess the quantitative reproducibility of the label-free quantification results in our single-run screening analysis, as well as the clinical usefulness of the 19 candidate biomarkers, we conducted further validation studies by multiple reaction monitoring (MRM) technology using 96 additional serum samples (**Table S1**). For designing the optimum MRM transitions specific

Table 1. 19 lung cancer biomarker candidates.

Expressionist ^a					MASCOT ^b			
Cluster ID ^c	m/z	RT	z	t-test p-value ^d	Acc. ^e	start	end	Peptide sequence
Cluster_3187	551.8	64.1	2	1.54E-15	ACCN4	613	624	CPSLGRAEGGGV
Cluster_3858	750.9	60.3	2	7.85E-04	APOA4	271	283	ELGGHLDQQVEEF
Cluster_3444	629.8	52.2	2	9.41E-07	APOA4	268	284	GGHLDQQVEEF
Cluster_3661	689.8	75.3	2	8.52E-08	APOA4	260	284	GNTGELQKSLAELGGHLDQQVEEFR
Cluster_3498	643.3	65.7	2	6.08E-05	APOA4	288	304	SLAELGGHLDQQVEEFR
Cluster_2454	756.4	65.6	3	2.93E-03	APOE	194	214	TVGSLAGQPLQERAQAWGERL
Cluster_248	768.8	53.0	2	6.41E-23	FIBA	1	16	ADSGEGDFLAEGGGVR
Cluster_126	432.7	62.6	2	3.07E-22	FIBA	7	15	DFLAEGGGV
Cluster_159	510.7	49.9	2	5.75E-25	FIBA	7	16	DFLAEGGGVR
Cluster_240	733.3	56.5	2	3.80E-15	FIBA	2	16	DSGEGDFLAEGGGVR
Cluster_166	525.7	62.8	2	2.99E-25	FIBA	5	15	EGDFLAEGGGV
Cluster_3342	603.8	50.7	2	8.17E-27	FIBA	5	16	EGDFLAEGGGVR
Cluster_2872	461.2	61.8	2	3.31E-12	FIBA	6	15	GDFLAEGGGV
Cluster_174	539.3	52.3	2	4.10E-15	FIBA	6	16	GDFLAEGGGVR
Cluster_180	554.2	63.5	2	5.37E-22	FIBA	4	15	GEGDFLAEGGGV
Cluster_207	632.3	52.1	2	1.98E-21	FIBA	4	16	GEGDFLAEGGGVR
Cluster_196	597.8	63.2	2	4.44E-24	FIBA	3	15	SGEGDFLAEGGGV
Cluster_221	675.8	52.3	2	2.22E-22	FIBA	3	16	SGEGDFLAEGGGVR
Cluster_135	453.2	39.0	2	2.81E-24	LBN	306	313	FLLSLVLT

^aInformation acquired from the Expressionist RefinerMS or the Analyst module.

^bInformation acquired from MASCOT database search.

^cEach ID corresponds to that in the bar chart (Fig. S1).

^dShown is the p-value of t-test between normal group and lung cancer group.

^eUniProt Accession Number.

doi:10.1371/journal.pone.0018567.t001

to the 19 candidate peptides, the m/z values of precursor ions detected in the screening phase were set as Q1 channels and those of four most intense fragment ions were selected from each MS/MS spectrum for Q3 channels (Fig. S2 and Table S3). Hence, a total of 76 MRM transitions were simultaneously monitored by 4000 Q1RAP mass spectrometry using a serum peptidome sample (Fig. 5). We then determined the specific eluting retention time for each candidate peptide and selected the optimum MRM transitions showing the highest MRM chromatogram peak out of four transitions for each peptide (Table S4). In our observations, only two peptides (FIBA 3 16 and FIBA 5 16) showed the identical orders of fragment ion intensities between QSTAR-Elite and 4000 Q1RAP systems as shown in Figure 5. We further performed MRM-based relative quantification analysis using 36 normal controls and 60 lung cancer samples in duplicated experiments. The serum levels of 19 candidate biomarker peptides were calculated on the basis of normalized and averaged MRM chromatogram peak areas and displayed with box plots (Fig. 6A). To evaluate the efficacy of these candidates for early detection of lung cancer, we compared the earlier-stage lung cancer group (stage-I, II, and IIIa) with the normal group by Student's t-test. The results revealed that 15 out of 19 candidate peptides showed significant differences in their serum levels between the two groups, while 4 peptides (FIBA 4 15, FIBA 5 15, FIBA 7 15, and FIBA 7 16) showed no significant differences. Concerning the comparison between the normal group and the advanced-stage lung cancer group (stage-IIIb and IV), similarly 4 peptides (APOA4 268 284, APOA4 271 283, FIBA 5 15, and APOE 194 214) did not satisfy the

criterion of $p < 0.05$. Hence, we considered that the remaining 12 peptides are likely to be more promising biomarkers for lung cancer diagnosis. We next assessed the sensitivity and specificity of the 19 biomarkers for lung cancer diagnosis by ROC curve analysis (Fig. 6B and Fig. S3). The cut-off value was set at the point whose distance from the (sensitivity, specificity) = (1, 1) reached the minimum. Given the value of sensitivity to detect lung cancer at an earlier stage, FIBA 6 15 (87.1%), APOA4 273 283 (61.3%), FIBA 5 16 (58.1%), and LBN 306 313 (58.1%) appeared to be the good biomarker candidates. However although the specificity of APOA4 273 283, FIBA 5 16, and LBN 306 313 were remarkably higher (88.9%, 94.4%, and 100%, respectively, Fig. 6B), FIBA 6 15 showed relatively lower specificity (44.4%) and the area under the curve (0.641). By integrating the results from t-test and ROC curve analysis, the 3 candidates shown in Figure 6B were considered as the most promising peptide biomarkers for early detection of lung cancer.

Discussion

Even though recent mass spectrometry instruments have allowed measurements of peptide mixtures at high sensitivity [24], enrichment of targeted proteins/peptides is still indispensable to achieving detection and identification of serum components in limited amounts of biological materials. In this sense, the methodology to purify preanalytical samples without loss of targeted components is crucial. From this point of view, the previous peptidome profiling technologies, such as SELDI-TOF-MS coupled with ProteinChip arrays or MALDI-TOF-MS

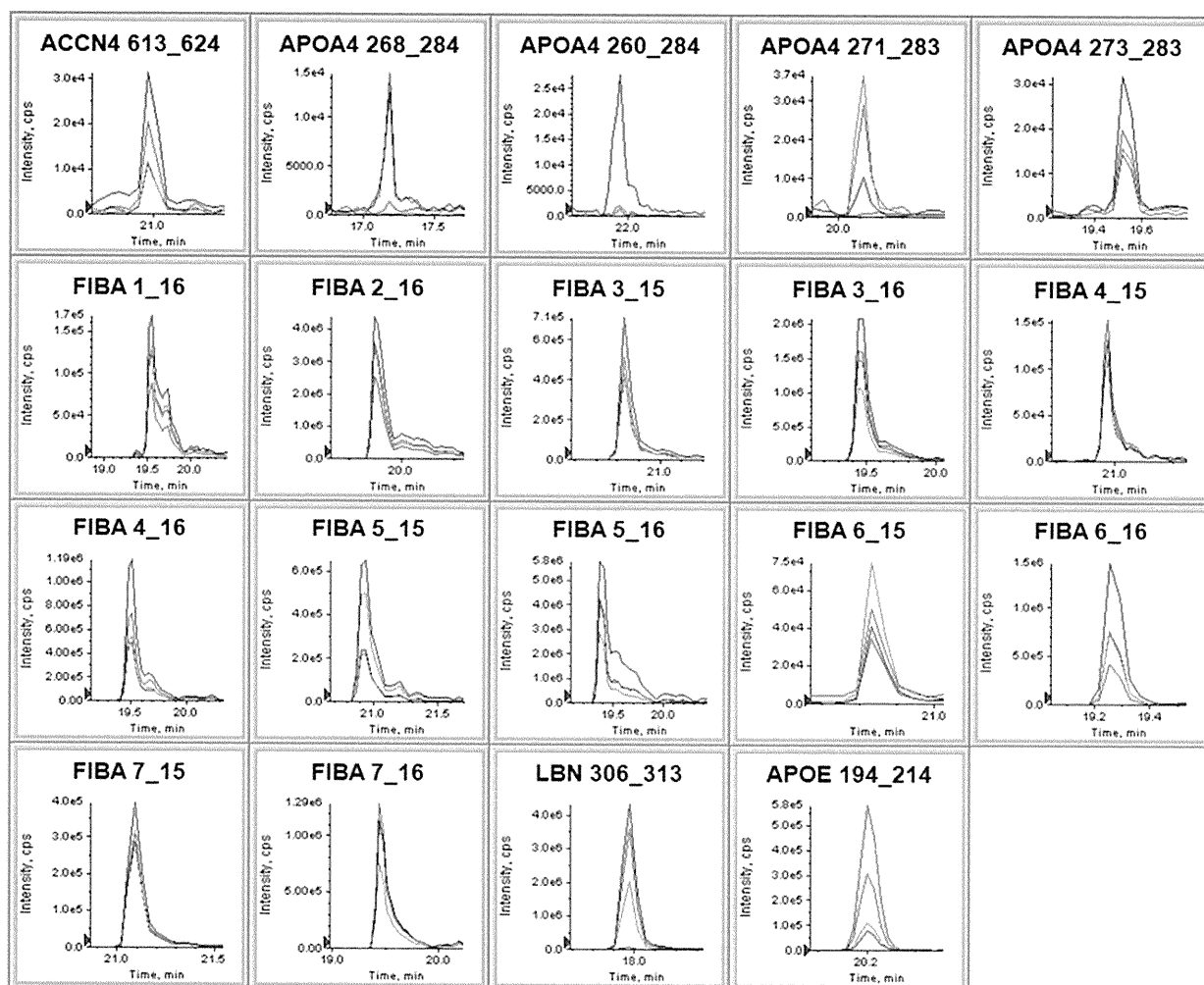


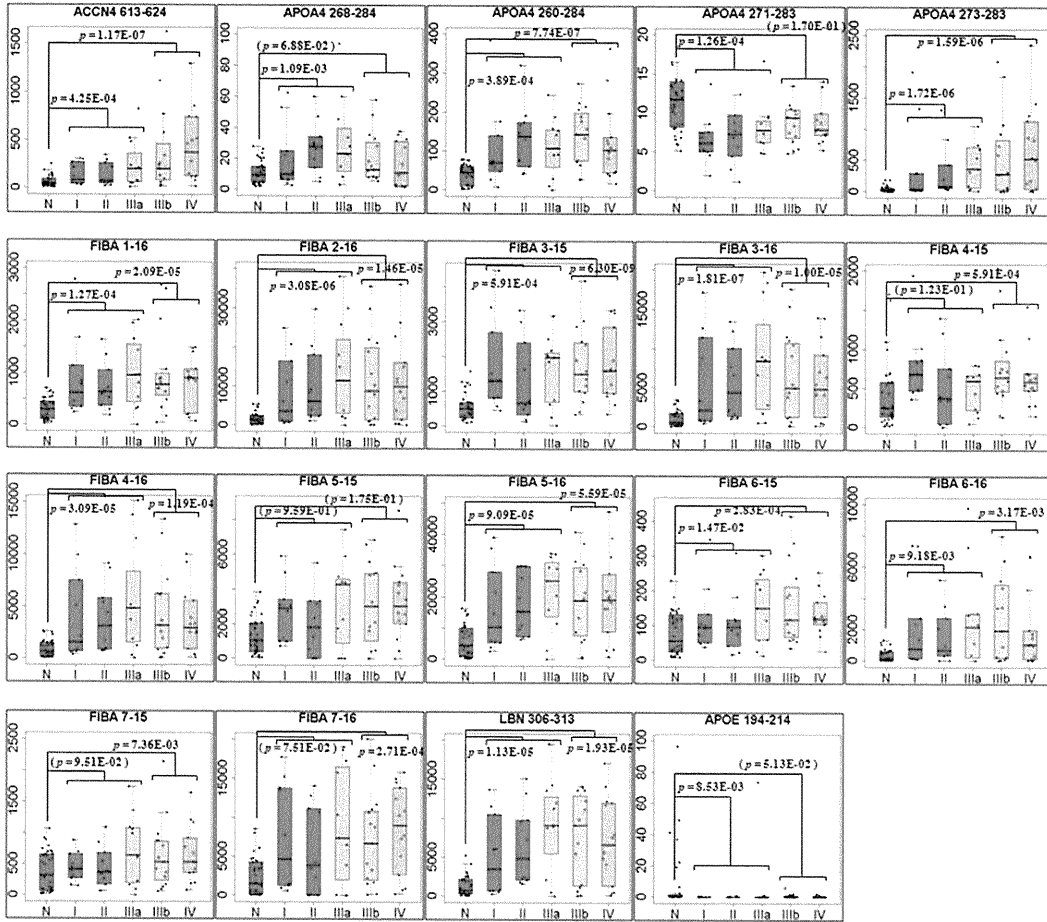
Figure 5. Selection and confirmation of the optimum MRM transitions for 19 candidates. Four pairs of precursor m/z and fragment m/z (Q1/Q3 channels) were set as MRM transitions for each peptide. The blue, red, green, or gray MRM chromatogram monitored the fragment ion which showed the 1st, 2nd, 3rd, or 4th most intense peaks in QSTAR-Elite LC/MS/MS analysis, respectively.
doi:10.1371/journal.pone.0018567.g005

analysis of ClinProt magnetic beads-purified samples, covered only limited spectra of serum peptidome. Most of studies utilizing ion-exchange selection or reversed phase extraction of peptidome on ProteinChip arrays [25,26,27] or magnetic beads [28,29] allowed at most 200 peak detections within the mass range 1,000 to 20,000. Meanwhile our peptidome profiling technology consisting of gel-filtration chromatography, custom-made high resolution C18 tip-column, QSTAR-Elite mass spectrometer, and Expressionist proteome server platform analysis enabled us to detect 12,396 non-redundant molecules with charge state of +1 to +10. The number of detected peaks here denoted the enormous advantage of our methodology for the analytical comprehensiveness compared to other existing methods. Although we focused on serum peptides involved in 3,537 clusters with charge stage of +2 to +6 in this study, 12,396 clusters might include non-peptide serum components such as metabolites, which should be also valuable for biomarker screening. Additionally, regarding the capacity of sample numbers to be analyzed simultaneously, the Expressionist server platform has a potential to handle a larger

number of clinical samples. Because we in fact needed only less than an hour to process 92 LC/MS/MS data in the Refiner MS module (Fig. 1A), a comprehensive analysis of up to 1,000 cases would be feasible in a day. Hence our peptidome profiling technology provides the outstanding features of data comprehensiveness and quantitative performance, which absolutely fit the in-depth screening of novel biomarkers from clinical samples such as serum and plasma compared to previous technologies described above, whereas estimating actual dynamic range of detected peptide concentrations would be needed by, for instance, MRM-based absolute quantification analysis in the future. It could be tailored to many diagnostic and pharmacodynamic purposes as comprehensive interpretations of catalytic and metabolic activities in body fluids or tissues.

By using this technology, we finally identified 19 serum peptides as candidate lung cancer biomarkers (Table 1). The subsequent MRM-based validation experiments and t-test resulted in the confirmation of 12 candidates as reliable lung cancer biomarkers (Fig. 6.4). Eight of them were fragments derived from fibrinopep-

A



B

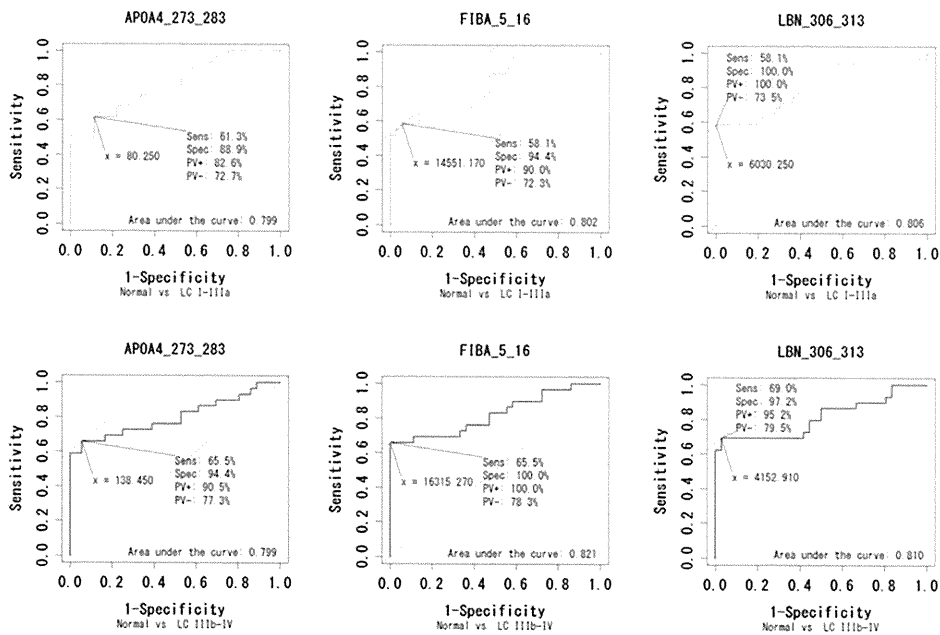


Figure 6. Statistical assessment of MRM-based validation experiments. (A) Box plots representing the stage-dependent distributions of serum levels of the 19 candidate biomarkers. The p-values from t-test between “normal group (n = 36) and lung cancer stage-I, II, and IIIa (n = 30)” or “normal group (n = 36) and lung cancer stage-IIIb and IV (n = 30)” are shown. The p-values that did not show significant differences were provided in parentheses. N: normal group, I, II, IIIa, IIIb, and IV: lung cancer stage-I, II, IIIa, IIIb, and IV group, respectively. (B) ROC curves for APOA4 206–284, FIBA 2–16, and LBN 306–313 were depicted by R. The green or blue graph shows comparison of “normal group (n = 36) and lung cancer stage-I, II, and IIIa (n = 30)” or “normal group (n = 36) and lung cancer stage-IIIb and IV (n = 30)”, respectively. The cut-off value was set at the point whose distance from the (sensitivity, specificity) = (1, 1) reached the minimum. The sensitivity (Sens), specificity (Spec), positive predictive value (PV+), negative predictive value (PV-), and area under the curve (AUC) were shown on each graph. doi:10.1371/journal.pone.0018567.g006

tide A (FPA) which is N terminally cleaved product from fibrinogen α (FIBA). In fact, both our screening and validation results suggested that all of these eight FPA fragments were potential lung cancer-associated biomarkers showing the significant increase of concentrations in lung cancer patients' sera. However, since anomalous turnover of FPA was previously reported in several other diseases including gastric cancer [30], diabetic nephropathy [31], coronary heart disease [32], and others, these 8 FPA fragments could not be defined as lung cancer-specific biomarkers. The other two candidates were generated from apolipoprotein A-IV (APOA4). APOA4 protein itself was already identified as an up-regulated biomarker for ovarian cancer [33], whereas this was also known to be regulated by nutritional and metabolic stress [34]. But both quantitative information and physiological functions of endogenously-processed APOA4 peptides in human serum were still unknown. Interestingly, the APOA4 273 283 fragment demonstrated pathological stage-dependent up-regulation in lung cancer patients' sera, while the two-residue longer fragment APOA4 271 283 was significantly decreased in lung cancer samples (Fig. 6A). This indicates the existence of lung cancer-associated endo- or exopeptidases responsible for the cleavage at the C-terminus of APOA4 a.a. 272. Additional two candidate biomarkers, LBN 306 313 and ACCN4 613 624, derived from limbin (LBN) and amiloride-sensitive cation channel 4 (ACCN4) proteins, were reported as cellular membrane proteins. LBN is also known as Ellis-van Creveld syndrome 2 (EVC2) that is expressed in the heart, placenta, lung, liver, skeletal muscle, kidney and pancreas. Defects in LBN (EVC2) are a cause of acrofacial dysostosis Weyers type (WAD, also known as Curry-Hall syndrome) [35]. ACCN4 is a newly identified member of the acid-sensing ion channel family expressed in pituitary gland and weakly in brain [36]. Neither of them was detected in serum previously. Since our study provided the first evidence of LBN 306 313 and ACCN4 613 624 detection in human serum, further analysis of physiological functions and measurement in other diseases should be required for the proper use in clinical lung cancer diagnosis. Hence, the three candidate biomarkers illustrated in Figure 6B (APOA4 273 283, FIBA 5 16, and LBN 306 313) were individually considered as clinically useful biomarkers for both early detection and tumor staging of lung cancer, however, integrative measurement of biomarkers such as Figure 4B would provide more accurate diagnosis, that could be achievable by MRM-based diagnostic approaches in the future. Consequently the sensitivity of these biomarkers was higher than the currently-used screening biomarker CEA especially at even stage-I or II [8], indicating that new biomarkers addressed in this study had great potential to realize the early detection system for lung cancer. However further validation experiments using high risk groups of lung cancer as the controls (such as heavy smokers or COPD patients) will be necessary to prove the specificity and clinical usefulness of our biomarkers because more practical target population of the early diagnosis of lung cancer should be them rather than healthy individuals.

Finally we grasped the birds-eye view of human peptidome as a snapshot of the specific disease state. We are recently willing to use

our peptidome profiling technology to establish an in-house quantitative serum/plasma peptidome database and contribute to the worldwide efforts such as Peptide Atlas (<http://www.peptideatlas.org/>). This framework would represent a new insight of protease/peptidase activities reflecting a clinical status at a specific time-point of disease and provide essential resources for next-generation extracorporeal diagnostic systems based on mass spectrometry. We therefore hope that researchers at global sites would utilize the peptidome profiling method addressed here and share data to construct mutually beneficial networks and databases which could contribute to the development of future diagnostic technologies worldwide.

Supporting Information

Figure S1 The bar charts illustrating the quantitative screening results for 19 candidates. The normalized peak intensities of 118 candidate biomarker peptides were calculated from 92 serum samples and displayed with bar charts. (TIFF)

Figure S2 MS/MS spectra used for the construction of MRM transitions and peptide identification. All MS/MS spectra were acquired with QSTAR-Elite mass spectrometer in the screening phase (the upper panels). The 1st, 2nd, 3rd, or 4th most intense peaks in each MS/MS spectrum were used for the optimization of MRM transitions (Fig. 5) The middle and the lower panels show the identified fragment ions in MASCOT database search. The ion scores and Expectation values were also indicated in the lower panels. (TIFF)

Figure S3 ROC curves for 19 lung cancer biomarker candidates were depicted by R. The green or blue graph shows comparison of “normal group (n = 36) and lung cancer stage-I, II, and IIIa (n = 30)” or “normal group (n = 36) and lung cancer stage-IIIb and IV (n = 30)”, respectively. The cut-off value was set at the point whose distance from the (sensitivity, specificity) = (1, 1) reached the minimum. The sensitivity (Sens), specificity (Spec), positive predictive value (PV+), negative predictive value (PV-), and area under the curve (AUC) were shown on each graph. (TIFF)

Table S1
(DOC)

Table S2
(DOC)

Table S3
(DOC)

Table S4
(DOC)

Acknowledgments

We thank Ms. Mari Kikuchi at AB Sciex for technical assistances.

Author Contributions

Conceived and designed the experiments: KU. Performed the experiments: KU NS ST DK AT. Analyzed the data: KU NS ST AT HN. Contributed

reagents/materials/analysis tools: AT YD NI NK KT TS MN T-AS YN HN. Wrote the paper: KU YN HN.

References

- Parkin DM (2001) Global cancer statistics in the year 2000. *Lancet Oncol* 2: 533–543.
- Samet JM, Avila-Tang E, Boffetta P, Hanman LM, Olivo-Marston S, et al. (2009) Lung cancer in never smokers: clinical epidemiology and environmental risk factors. *Clin Cancer Res* 15: 5626–5645.
- Goldstraw P, Crowley J, Chansky K, Giroux DJ, Groome PA, et al. (2007) The IASLC Lung Cancer Staging Project: proposals for the revision of the TNM stage groupings in the forthcoming (seventh) edition of the TNM Classification of malignant tumours. *J Thorac Oncol* 2: 706–714.
- Henschke CI, Yankelevitz DF, Libby DM, Pasmantier MW, Smith JP, et al. (2006) Survival of patients with stage I lung cancer detected on CT screening. *N Engl J Med* 355: 1763–1771.
- Gail MH, Muenz L, McIntire KR, Radovich B, Braunstein G, et al. (1988) Multiple markers for lung cancer diagnosis: validation of models for localized lung cancer. *J Natl Cancer Inst* 80: 97–101.
- McCarthy NJ, Swain SM (2001) Tumor markers: should we or shouldn't we? *Cancer J* 7: 175–177.
- Brundage MD, Davies D, Mackillop WJ (2002) Prognostic factors in non-small cell lung cancer: a decade of progress. *Chest* 122: 1037–1057.
- Sung HJ, Cho JY (2008) Biomarkers for the lung cancer diagnosis and their advances in proteomics. *BMB Rep* 41: 615–625.
- Maurya P, Mcleady P, Dowling P, Clynes M (2007) Proteomic approaches for serum biomarker discovery in cancer. *Anticancer Res* 27: 1247–1255.
- Gamez-Pozo A, Sanchez-Navarro I, Nistal M, Calvo E, Madero R, et al. (2009) MALDI profiling of human lung cancer subtypes. *PLoS One* 4: e7731.
- Wollscheid B, Bausch-Fluck D, Henderson C, O'Brien R, Bibel M, et al. (2009) Mass-spectrometric identification and relative quantification of N-linked cell surface glycoproteins. *Nat Biotechnol* 27: 378–386.
- Schiess R, Wollscheid B, Aebersold R (2009) Targeted proteomic strategy for clinical biomarker discovery. *Mol Oncol* 3: 33–44.
- Ueda K, Takami S, Saichi N, Daigo Y, Ishikawa N, et al. (2010) Development of serum glycoproteomic profiling technique; simultaneous identification of glycosylation sites and site-specific quantification of glycan structure changes. *Mol Cell Proteomics* 9: 1819–1828.
- Ostroff RM, Bigbee WL, Franklin W, Gold L, Mehan M, et al. (2010) Unlocking biomarker discovery: large scale application of aptamer proteomic technology for early detection of lung cancer. *PLoS One* 5: e15003.
- Villanueva J, Nazarian A, Lawlor K, Tempst P (2009) Monitoring peptidase activities in complex proteomes by MALDI-TOF mass spectrometry. *Nat Protoc* 4: 1167–1183.
- Shen Y, Tolic N, Liu T, Zhao R, Petritis BO, et al. (2010) Blood peptidome-degradome profile of breast cancer. *PLoS One* 5: e13133.
- Lopez-Otin C, Bond JS (2008) Proteases: multifunctional enzymes in life and disease. *J Biol Chem* 283: 30433–30437.
- Overall CM, Blobel CP (2007) In search of partners: linking extracellular proteases to substrates. *Nat Rev Mol Cell Biol* 8: 245–257.
- Palermo C, Joyce JA (2008) Cysteine cathepsin proteases as pharmacological targets in cancer. *Trends Pharmacol Sci* 29: 22–28.
- Lopez-Otin C, Matrisian LM (2007) Emerging roles of proteases in tumour suppression. *Nat Rev Cancer* 7: 800–808.
- Egeblad M, Werb Z (2002) New functions for the matrix metalloproteinases in cancer progression. *Nat Rev Cancer* 2: 161–174.
- Albrethsen J, Bogebo R, Gammeltoft S, Olsen J, Winther B, et al. (2005) Upregulated expression of human neutrophil peptides 1, 2 and 3 (HNP 1-3) in colon cancer serum and tumours: a biomarker study. *BMC Cancer* 5: 8.
- Sasaki K, Takahashi N, Satoh M, Yamasaki M, Minamino N (2010) A peptidomics strategy for discovering endogenous bioactive peptides. *J Proteome Res* 9: 5047–5052.
- Anderson NL, Anderson NG, Pearson TW, Borchers CH, Paulovich AG, et al. (2009) A human proteome detection and quantitation project. *Mol Cell Proteomics* 8: 883–886.
- Liu M, Li CF, Chen HS, Lin LQ, Zhang CP, et al. (2010) Differential expression of proteomics models of colorectal cancer, colorectal benign disease and healthy controls. *Proteome Sci* 8: 16.
- Qiu FM, Yu JK, Chen YD, Jin QF, Sui MH, et al. (2009) Mining novel biomarkers for prognosis of gastric cancer with serum proteomics. *J Exp Clin Cancer Res* 28: 126.
- Wang Q, Shen J, Li ZF, Jie JZ, Wang WY, et al. (2009) Limitations in SELDI-TOF MS whole serum proteomic profiling with IMAC surface to specifically detect colorectal cancer. *BMC Cancer* 9: 287.
- Wong MY, Yu KO, Poon TC, Ang IL, Law MK, et al. (2010) A magnetic bead-based serum proteomic fingerprinting method for parallel analytical analysis and micropreparative purification. *Electrophoresis* 31: 1721–1730.
- Huang Z, Shi Y, Cai B, Wang L, Wu Y, et al. (2009) MALDI-TOF MS combined with magnetic beads for detecting serum protein biomarkers and establishment of boosting decision tree model for diagnosis of systemic lupus erythematosus. *Rheumatology (Oxford)* 48: 626–631.
- Ebert MP, Niemeyer D, Deininger SO, Wex T, Knippig C, et al. (2006) Identification and confirmation of increased fibrinopeptide a serum protein levels in gastric cancer sera by magnet bead assisted MALDI-TOF mass spectrometry. *J Proteome Res* 5: 2152–2158.
- Gianazza E, Mainini V, Castoldi G, Chinello C, Zerbini G, et al. (2010) Different expression of fibrinopeptide A and related fragments in serum of type 1 diabetic patients with nephropathy. *J Proteomics* 73: 593–601.
- Zito F, Drummond F, Bujac SR, Esnouf MP, Morrissey JH, et al. (2000) Epidemiological and genetic associations of activated factor XII concentration with factor VII activity, fibrinopeptide A concentration, and risk of coronary heart disease in men. *Circulation* 102: 2058–2062.
- Dieplinger H, Ankerst DP, Burges A, Lenhard M, Lingenhel A, et al. (2009) Afamin and apolipoprotein A-IV: novel protein markers for ovarian cancer. *Cancer Epidemiol Biomarkers Prev* 18: 1127–1133.
- Hanniman EA, Lambert G, Inoue Y, Gonzalez EJ, Sinal CJ (2006) Apolipoprotein A-IV is regulated by nutritional and metabolic stress: involvement of glucocorticoids, HNF-4 alpha, and PGC-1 alpha. *J Lipid Res* 47: 2503–2514.
- Galdzicka M, Patnala S, Hirshman MG, Cai JF, Nitowsky H, et al. (2002) A new gene, EVC2, is mutated in Ellis-van Creveld syndrome. *Mol Genet Metab* 77: 291–295.
- Grunder S, Geissler HS, Bassler EL, Ruppertsberg JP (2000) A new member of acid-sensing ion channels from pituitary gland. *Neuroreport* 11: 1607–1611.